Introduction

Hip pain is a common and disabling condition that affects patients of all ages. The differential diagnosis of hip pain is broad, presenting a diagnostic challenge. Magnetic resonance imaging is valuable for the detection of occult traumatic fractures, stress fractures, and osteonecrosis of the femoral head[1].

Avascular necrosis of the femoral head is an increasingly common cause of musculoskeletal disability, and it poses a major diagnostic and therapeutic challenge. The disease affects mostly young adults within their 3rd and 5th decade, the majority of the patients being men[2].

MRI has become the imaging modality of choice, as it is highly sensitive and specific for osteonecrosis. T1W images on MRI typically demonstrate a serpiginous "band like" lesion with low signal intensity in the anterosuperior femoral head, and a "double- line sign" can be seen on T2 sequences[3].

MR imaging is a valuable tool in the diagnosis of early or radiographically occult Legg-Calvé-

Perthes disease. It shows the extent of epiphyseal involvement[4].

Occult fractures in the elderly are one of the most frequent indications for MRI of the hip. In these generally osteoporotic patients, plain films may not demonstrate the fracture line, and bone scintigraphy may demonstrate increased uptake only several days after the trauma. MRI is highly sensitive for detecting the fracture and the surrounding edema immediately after the traumatic event[5].

The key MR imaging features of rapidly destructive hip osteoarthritis include an extensive bone marrow edema like pattern in the femoral head and neck, femoral head flattening, and cyst-like subchondral defects. Additional findings include epiphyseal low-signal-intensity lines, band-like areas of low signal intensity in the subchondral bone of the femoral head [6].

Transient osteoporosis of the hip is an uncommon cause of hip pain, mostly affecting healthy middle-aged men and also women in the third trimester of pregnancy[7].

MRI of congenital dislocation of the hip has several advantages: it is non-invasive, harmless, painless, and involves no ionizing radiation. MRI also provide anatomical images in several cross-sections[(8)].

MRI of the hip is not only useful to confirm successful reduction but may also help to predict outcome by evaluating following dislocation[(9)].

Aim Of The Work

The aim of this work is to assess the role of magnetic resonance imaging in diagnosis of non-neoplastic femoral head lesions.

GROSS ANATOMY OF THE HIP JOINT

Embryology & early development of the hip joint:

The child's hip begins in intrauterine development as a condensation of mesoderm in the lower limb bud that rapidly differentiates to resemble the adult hip by eight weeks of life[10].

The lower limb bud develops as an outgrowth from
the ventral surface of the embryonic mass at approximately 4 weeks' gestational age. The club-shaped femoral pre-cursors along with the iliac, ischial and pubic pre-modal centers develop at around 6 weeks. Between 6 and 11 weeks the femoral head can be identified as a mass of cells interposed between the distal femur and the pelvis, at the same time the primitive femoral neck and greater trochanter form. Cavitation occurs between this cell mass and the femur creating the joint space. Any abnormality present at birth is therefore secondary to abnormal development from 11 weeks

onwards. After 11 weeks vascular invasion, cartilage formation and ligament development become apparent. The hip joint is completely developed by 5 months of gestational age[11].

Following birth ossification of the proximal femoral epiphysis is generally seen in girls between 2 and 6 months of age and in boys between 3 and 7 months. Femoral head ossification is seen in 50% of children by4months and in90%by7monthsof age[11].

Anatomy

The hip joint is a ball and socket joint, formed by femoral head and the acetabulum. The articular surfaces are spherical with a marked congruity, it limits the range of movement but contributes to the considerable stability of the joint[12].

The hip joint exhibits a very effective compromise between mobility and stability, allowing movement in all three orthogonal planes[13].

The femoral head faces antero-supero-medially to articulate with the acetabulum. The head, (fig.1) often described as rather more than half a 'sphere',

is not part of a true sphere but is spheroidal and is part of the surface of an ovoid. Its smoothness is interrupted postero-inferior to its centre by a small, rough fovea. The head is intracapsular, the distal half is encircled by the acetabular labrum. Its periphery is distinct, except anteriorly, where the articular surface extends to the neck. The ligamentum teres attaches to the fovea. The anterior surface of the head is separated inferomedially from the femoral artery by the tendon of psoas major, the psoas bursa, and the articular capsule[13].

1.Trochanteric fossa. 2. Greater trochanter. 3. Quadrate tubercle.

4. intertrochanteric crest. 5. Gluteal tuberosity. 6. Linea aspera.

7.fovea of ligamentum teres attachment. 8. Lesser trochanter

9. Spiral line.

Figure (1): Proximal end of femur: posterior aspect[13].

The femoral head is completely cartilaginous at birth, and the greater trochanter is part of this same cartilaginous block. The femoral neck begins to form only after birth and a thin cartilaginous connection between the head and the trochanters remains at least into infancy. As in the acetabulum, the thin articular surface of the femoral head is hyaline cartilage supported by a mass of growth cartilage[14].

The growth cartilages of the femoral head and the acetabulum, as well as the bony femoral epiphysis, are vascularized by small, nonanastomotic end arteries lying within cartilage canals. These vessels can be compromised during treatment of congenital dislocation, leading to avascular necrosis[14].

The acetabulum is formed by fusion of the three bones. Ilium, Ischium and pubis meet at a "Y" shaped cartilage. The acetabular articular surface is incomplete cartilaginous ring on the head of the femur, thicker at the center than that at the circumference, covers the entire surface with the exception of the fovea capitis fermoris, to which the ligamentum teres is attached[(14)].

The peripheral edge of the acetabulum is deepened by a rim of dense fibrous tissue, which encloses the femoral head beyond its equator, increasing the stability of the joint. This rim is named the labrum acetabulare, and it is continued across the acetabular notch to produce the transverse ligament that gives attachment to ligamentum teres. The center of non-articular part of the acetabulum is occupied by a pad of fat known as Haversian pad [(14)] (fig.2).

The appearance of marrow is dependent on the age of the patient, specifically the relation of yellow or fatty marrow to that of red or hematopoietic marrow[(15)].

In a fetus and at the time of birth, all bone

marrow is hematopoietic. Subsequently, there is organized conversion to yellow marrow, beginning in epiphyses of the femur, which generally occurs by 1 year of age(15).

The femoral diaphysis is the next region to undergo conversion, and there is progression of conversion toward the metaphyseal regions. In the adult, most of the marrow within the femur is fatty; however, if hematopoietic marrow is present, it is generally restricted to the proximal femoral metaphysis(15).

In the pelvis, hematopoietic marrow is diffusely distributed, with areas of focal fatty marrow found around the sacroiliac joints, acetabula, and symphysis pubis. This hematopoietic marrow may become more prominent or may be replaced by fatty marrow as the patient ages. These changes tend to be bilateral and symmetric(15).

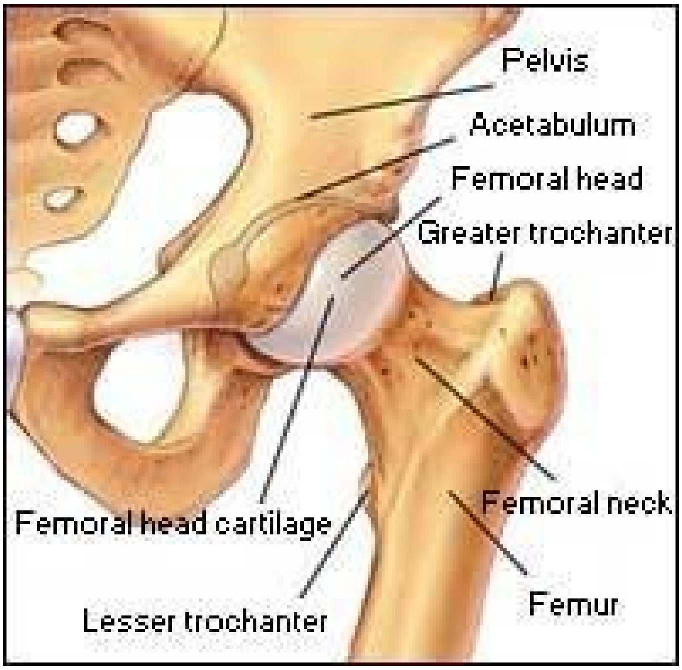

Figure (2): Hip joint articular surfaces[16].

The ligamentum teres plays only a minor role in the control of hip movement. Adduction from a semi-flexed position is the only movement where this ligament is under tension. The thickness of the femoral head cartilage is 3mm posteriorly and superiorly and 0.5mm along the periphery and inferior margin [17].

The capsule is cylindrical sleeve, running from the acetabular rim to the base of the neck. It is strong and dense and it is attached circumferentially around the labrum acetabulare

and transverse ligament. it is connected to the transverse ligament by a few fibers to the edge of the obturator foramen and surrounds the neck of the femur (fig.3)[18].

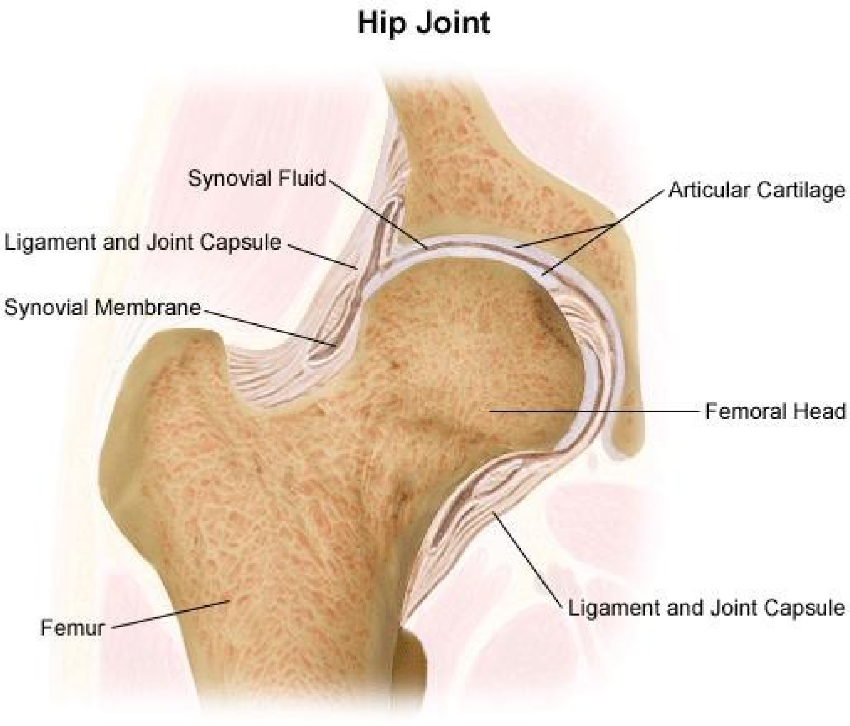

Figure (3): The gross anatomy of the joint capsule[18].

The capsule consists of two sets of fibers, circular and longitudinal. The circular fibers, Zona orbicularis, are most abundant at the lower and the posterior part of the capsule and form a sling around the neck of the femur. The longitudinal fibers are greatest in amount at the upper and front

part of the capsule, where they are reinforced by accessory ligaments[18].

The synovial membrane lines the entire capsule, invests the retinacular fibers and forms a sleeve around the Haversian pad and ligamentum teres. Occasionally a perforation in the anterior part of the capsule permits communication between the synovial cavity and the iliac bursa[19].

The inelastic fibrous capsule of the hip is reinforced by iliofemoral, pubofemoral and ischeofemoral ligaments. The iliofemoral ligament is the strongest and thickest capsular ligament. It lies in front of the joint and intimately connected with the capsule. It is attached, above to the lower part of the anterior inferior iliac spine; below, it divides into two bands, one of which passes downward to the lower part of the intertrochanteric line; the other is directed downward and laterally to attach to the upper part of the same line[20].

The pubofemoral ligament is attached above to the obturator crest and the superior ramus of the pubis; below, it blends with the capsule and with the deep surface of the vertical band of the

iliofemoral ligament. The ischiofemoral ligament consists of a triangular band of strong fibers, which spring from the ischium below and behind the acetabulum, and blend with the circular fibers of the capsule (fig.4)[13].

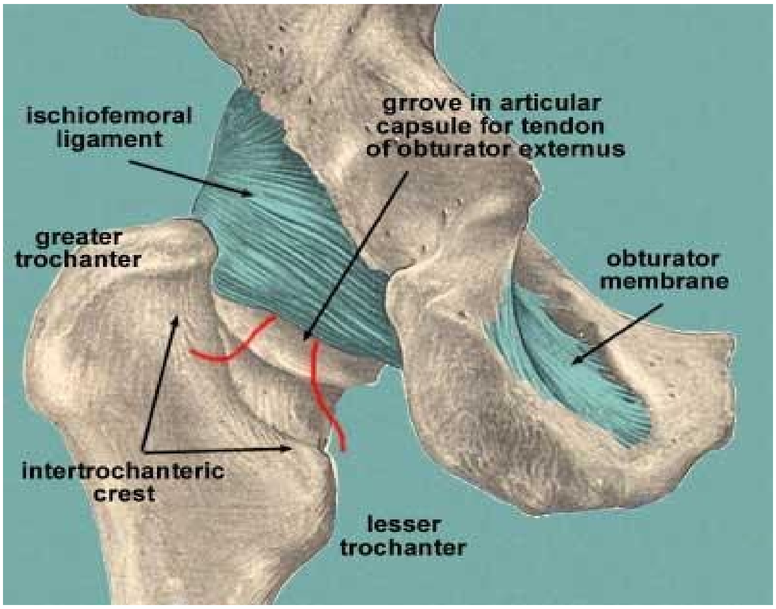

Figure (4): The ischiofemoral ligament[13].

Muscles of the Hip

Movements of the hip joint can be categorized as flexion-extension, adduction-abduction, medial and lateral rotation [13] (Fig. 5) .

Flexion is produced by psoas major and iliacus, assisted by pectineus, rectus femoris and sartorius. The adductors, particularly adductor longus, also assist, especially in early flexion from

full extension)[13].

Extension is produced by gluteus maximus and the hamstring (posterior femoral)muscles. The rate of change of posture, is largely controlled by the hamstrings which, although powerful flexors of the knee, are equally strong extensors of the hip. Gluteus maximus only becomes active when the thigh is extended against resistance, as in rising from a bending position or climbing)[13].

Abduction is produced by gluteus medius and minimus, assisted by tensor fasciae latae and sartorius. Abduction is limited by adductor tension, the pubofemoral ligament and the medial band of the iliofemoral ligament. These muscles are consistently involved in walking or running, contracting periodically at precise phases of the walking or running cycle)[13].

Adduction is produced by adductors longus, brevis and magnus, assisted by pectineus and gracilis. Adduction is limited by contact with the opposite limb but its range is wider with the thigh flexed, when it is limited by the abductor muscles, the lateral band of the iliofemoral ligament and

ligament of the femoral head)[13].

Medial rotation is produced by tensor fasciae latae and the anterior fibres of gluteus minimus and medius. It is relatively weak and is limited by the lateral rotators, ischiofemoral ligament and the posterior part of the capsule. Electromyographic data suggest that the adductors usually assist in medial rather than lateral rotation, but this is, of course, dependent on the primary position)[13].

Lateral rotation is produced by the obturator muscles, the gemelli and quadratus femoris, assisted by piriformis, gluteus maximus and sartorius. It is a powerful action and limited by tension in the medial rotators and the lateral band of the iliofemoral ligament) [13].

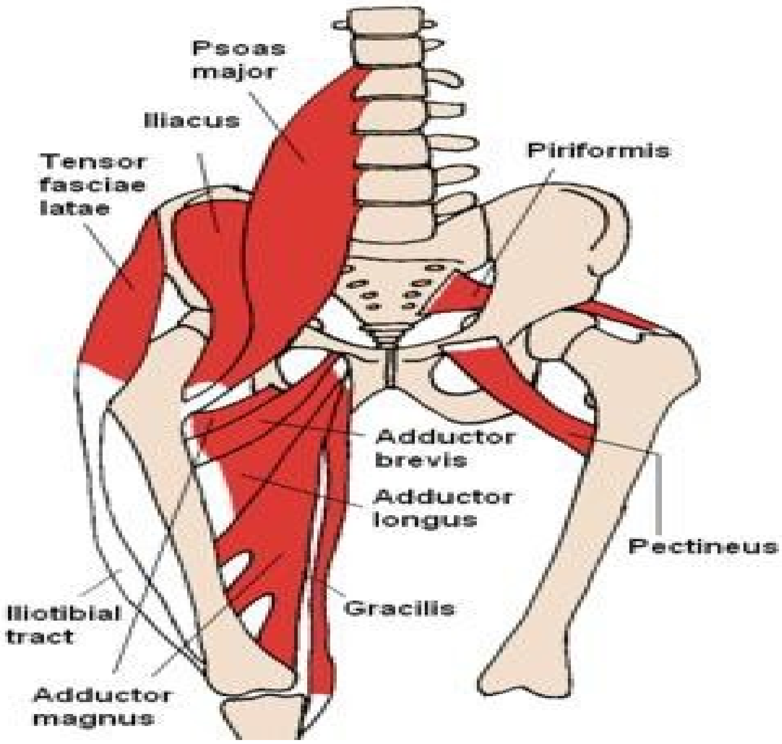

Figure (5): Muscles around the hip joint[20].

Blood Supply:

The vascular anatomy of the femoral head is very specific
because the vascular patterns established during the growth
phases do not change at maturity and persist throughout life [21].

There are three main sources of blood to the proximal femur: an extracapsular arterial ring, the

ascending cervical (retinacular branches) vessels, and the artery of the ligamentum teres (Fig. 6&7). The extracapsular ring is formed mostly by the medial and lateral femoral circumflex vessels. This ring gives rise to the ascending cervical branches, which are extracapsular, and these in turn give rise to the metaphyseal and epiphyseal branches. The anterior portion of the extracapsular ring is formed primarily by the lateral femoral circumflex artery. The posterior, lateral, and medial aspects of the ring are formed by the medial femoral circumflex artery[22]

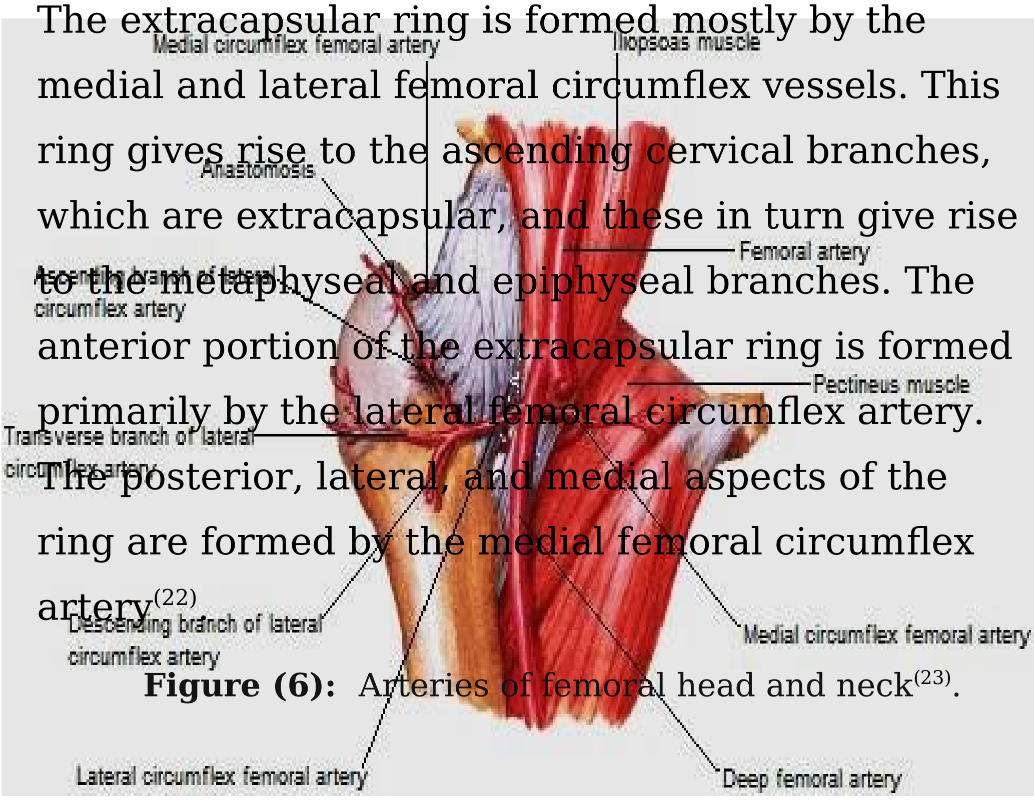

Figure (6): Arteries of femoral head and neck[23].

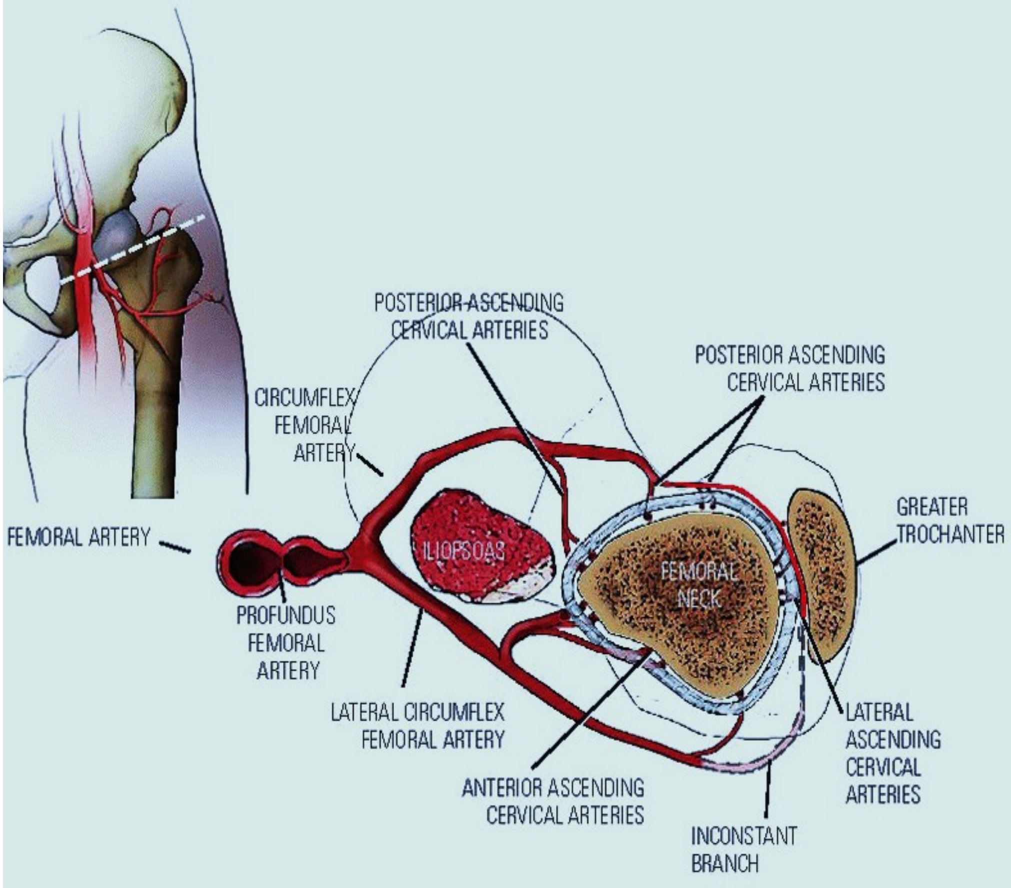

Figure (7): The blood supply to the normal proximal femur in a child[22].

Observations on developmental patterns of the blood supply of femoral head in late fetal and early postnatal periods have revealed that although medial and lateral circumflex femoral arteries at first contribute equally, two major branches of the medial provide the final supply, both posterior to the neck. The supply from the lateral circumflex artery diminishes and the arterial ring is

interrupted. As the femoral neck elongates, the extracapsular circle becomes more distant from the epiphysial part of the head[13].

Venous Drainage:

The pattern of venous drainage of the head and neck of the femur corresponds in general to that of the arteries, though there may be a single large cervical vein postero-inferiorly[13].

Lymphatic Drainage of the lower limb: [13]

Lymphatic drainage of superficial tissues

The superficial lymph vessels begin in subcutaneous plexuses Collecting vessels leave the foot medially, along the long saphenous vein, or laterally with the short saphenous vein. Medial vessels are larger and more numerous. They start on the tibial side of the dorsum of the foot, and ascend anterior or posterior to the medial malleolus. Thereafter both sets converge on the long saphenous vein and accompany it to the distal superficial inguinal nodes. Lateral vessels begin on the fibular side of the dorsum of the foot, and some cross anteriorly in the leg to join the medial vessels and so pass to the distal superficial

inguinal lymph nodes. Others accompany the short saphenous vein to the popliteal nodes. Superficial lymph vessels from the gluteal region run anteriorly to the proximal superficial inguinal nodes.

Lymphatic drainage of deeper tissues:

The deep vessels accompany the anterior and posterior tibial, peroneal, popliteal and femoral vessels. The deep vessels from the foot and leg are interrupted by popliteal nodes; those from the thigh pass to the deep inguinal nodes. The deep lymph vessels of the gluteal and ischial regions follow their corresponding blood vessels. Those accompanying the superior gluteal vessels end in a node near the intrapelvic part of the superior gluteal artery, near the superior border of the greater sciatic foramen, while those which follow the inferior gluteal vessels traverse one or two of the small nodes below piriformis and pass to the internal iliac nodes.

Nerve Supply:

The hip joint is supplied by articulator branches from sacral plexus, sciatic, obturator,

accessory obturator nerves and a filament from the branch of the femoral nerve supplying the rectus femoris[24].

Radiological and medical imaging techniques in examination of the hip joint:

● ***X-ray:*** *It* remains the initial tool for evaluation of the majority of musculoskeletal conditions involving the hip and pelvis. These include acute and chronic injury, infection, avascular necrosis, arthritis, metabolic disease, tumor, and dysplasia[25].

In plain radiography (X-ray), anteroposterior and lateral hip radiographs are usually taken(Fig. 8: A&B) . An anteroposterior hip radiograph includes images of both sides of the hip on the same film and

projects towards the middle of the line connecting the upper symphysis pubis and anterior-superior iliac spine; the distance between the X-ray tube and the film should be 1.2 m. If anteroposterior hip radiographs are taken in a supine position, one of the most common mistakes is image distortion as the hip is externally rotated. Thus, either both patellae should be facing forward or lower extremities should be internally rotated by 15°-20° to accommodate femoral anteversion in anteroposterior hip radiographs[26].

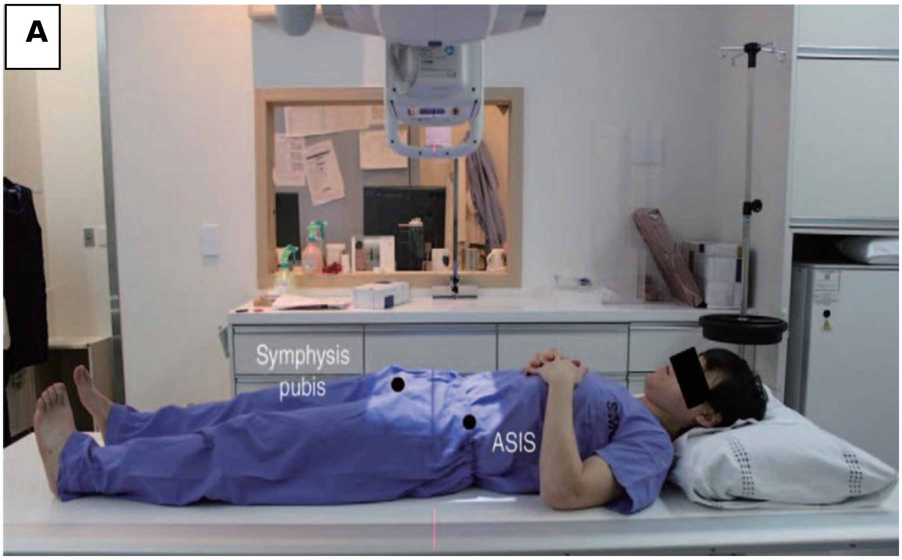

B

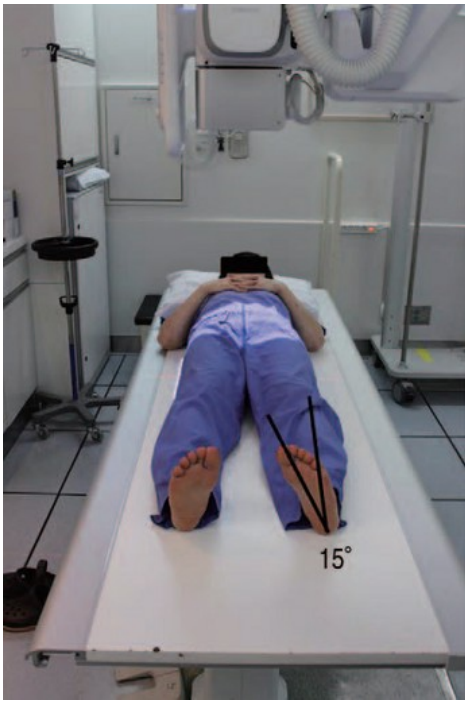

Figure 8 (A&B): Positioning for an anteroposterior hip radiograph(26).

There are multiple imaging techniques for lateral hip radiography, including the frog-leg lateral view, Löwenstein view, and cross-table lateral view. In the frog-leg lateral view, both sides are shown on one image and the knee joint is flexed 30□ -40□ in a supine position, while the hip is externally rotated by 45□so that the image is taken toward the middle of the line connecting the upper symphysis pubis and the anterior-superior iliac spine (Fig. 9) (26).

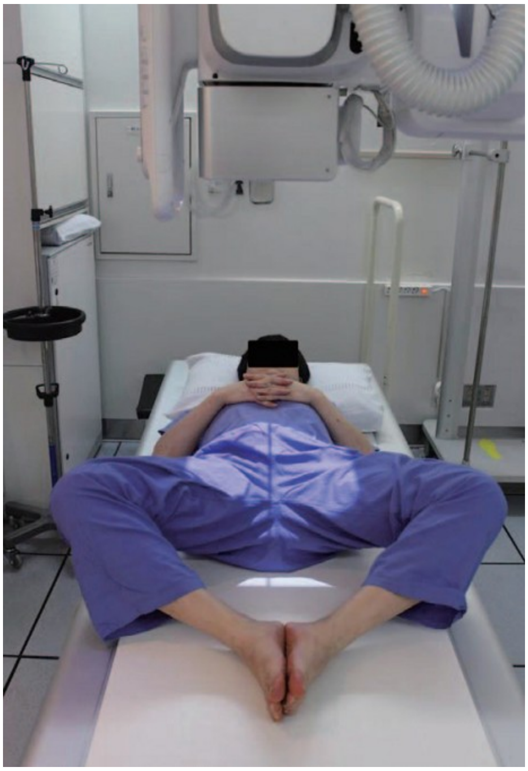

Figure (9): Positioning for a frog-leg lateral view[26].

● ***Computed tomography:*** In the setting of acute trauma, CT is essential for diagnosis of subtle fractures and for planning surgical intervention. It offers advantages over radiography in some situations, as when evaluating cortices, avulsions, matrix mineralization, and soft tissue calcifications[25].

CT technique has an intrinsic high spatial resolution and is more sensitive than X-ray in detecting bone typical osteonecrosis abnormalities, but it is still focused on the late stage of the

disease. There are several proposed acquisition protocols, all characterized by a low slice thickness (1–2 mm) and pitch (1–1.5 mm). Commonly used image matrix is 512 × 512 and is usually associated to a reduced field of view. Multiplanar reformats (like coronal and sagittal sections) associated with bone filtering are mandatory and possibly increase the accuracy in evaluating the articular surface.[25]

● ***Magnetic resonance imaging:*** It is the best test for detection of fracture as well as for the associated soft tissue injury. MRI is also excellent for diagnosis of stress-related injuries, which may not be apparent radiographically. In its early stages, AVN of the femoral head is also not visualized on radiographs. MRI is highly sensitive and can guide rapid intervention such as core decompression. It is also the test of choice for infection because it can give an overall picture of soft tissue disease and spread as well as underlying osseous involvement. MR arthrography is the test of choice for detection of acetabular labral tear[25].

● ***Musculoskeletal ultrasound:*** It is the primary choice to use for the detection of DDH in the

neonatal hip also can determine the characteristics of an effusion or guide an aspiration procedure[25].

Over the last decade, US has proven to be a useful tool in the assessment of tendons, ligaments, muscles, nerves, synovial recesses, articular cartilage, bone surfaces and joint capsule. The goals of US imaging are to detect and localize pathological processes, to differentiate between intraarticular and extraarticular pathology, to perform diagnostic and therapeutic interventional procedures and to monitor the efficacy of the therapy[27].

The routine scanning technique for US examination should consider the anterior, medial, lateral and posterior aspects of the hip as separate quadrants. Ultrasound equipment with multi-frequency linear transducer (5.0- 12.5 MHz) can provide a general evaluation of musculoskeletal structures. Superficial structures are well visualized with linear multi-frequency 9-15-MHz transducers. Higher frequency probes provide better spatial resolution but with a limitation because of less penetration. For children examination 10-14 MHz

transducers are recommended due to the relatively superficial position of the hip joint. When inflammatory pathology is suspected, Doppler techniques should be used for the evaluation of increased local perfusion considering that Doppler signal is detected with difficulties in deep areas[27].

The correct transducer position in relation to the underlying structure to be examined is the key element in achieving a good diagnostic image. Examination of the contralateral hip is advisable for comparison. (Table 1) shows the appropriate scans for the assessment of the hip joint and periarticular soft tissues[27].

Table (1) : Ultrasonography scans of the hip[27]:

Anterior examination
Anterior recess of the hip Bony profile Anterior regional muscles
Medial examination
Insertion of the iliopsoas tendon Pelvic insertion of the adductor muscles
Lateral examination
Greater trochanter Gluteus minimus and medius tendons Fascia latae
Posterior examination
Ischial tuberosity Hamstrings and sciatic nerve

●***Bone scan:*** It can be useful for screening for avascular
necrosis (AVN), evaluation of suspected stress fracture, prosthesis loosening, osteomyelitis (in conjunction with labeled-WBC scan), and tumor (to differentiate benign from malignant sclerotic lesions or to look for multiplicity of lesions) [25].

Nuclear medicine techniques, such as bone scan, SPECT, SPECT/CT and PET or PET/CT are not routinely used in AVN patients and their role is still under investigation. Osteonecrosis areas appear as photopenic lesions circumscribed by a reactive (hot)

interface (bull's eye sign) at 99 technetium bone scan. Although this technique has been demonstrated to be more sensitive than plain films and particularly suitable for non-cooperative patients in early stages, its performance against MRI was unsatisfactory, with only 56% of sensitivity compared to 100% sensitivity of the latter. Recently, SPECT/CT was also used in treatment follow-up to determine the viability of the graft after Vascularized Fibular Grafting intervention which is characterized by a time dependent increase of tracer uptake suggesting revascularization. [35]

NORMAL MAGNETIC RESONANCE ANATOMY OF THE HIP JOINT

MRI proved to be highly accurate imaging modality allows clear differentiation of the normal anatomic features of the hip .Also it allows clear differentiation of the individual component of the normal joint from one another. In addition, MRI allows identification of the bone marrow, cortex, muscles, fascia, nerves and vessels with high contrast between these structures[28].

Axial Images:

The axial plane displays the relationship between the femoral head and the acetabulum with supporting musculature.

At the level of the acetabular roof (fig. 10), the axial images may show a partial volume effect with the femoral head. The hip musculature demonstrates intermediate signal intensity on T1-weighted images. The gluteal muscles can be differentiated from one another by high signal intensity fat along fascial divisions. The tensor fascia latae muscle is seen anterior to the gluteus medius and is bordered

anteriorly by subcutaneous fat. The iliopsoas muscle group is anterior to the femoral head. The Sartorius muscle is the most anterior, and the rectus femurs is positioned between the more lateral tensor fasciae latae and the medial iliopsoas. The obturator internus muscle is visualized medial to the anterior and posterior acetabular columns [29].

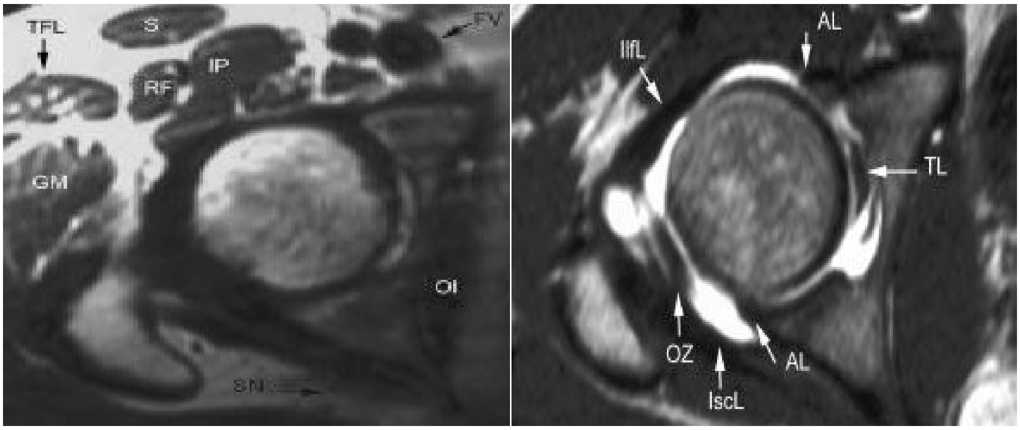

Figure (10): MR axial T1WI at the level of the of the acetabulum , (A) without and (B) with intra-articular injection of gadolinium. As well as the labrum. FV = femoral vessels; IP = iliopsoas muscle; S = sartorius muscle; RF = rectus femoris muscle; TFL = tensor fascia lata; GM = gluteus maximus muscle; OI: obturator internus muscle; SN = sciatic nerve; TL = teres ligament; AL = acetabular labrum; IlfL = iliofemoral ligament;OZ = orbicular zone; IscL: ischiofemoral ligament[29] .

Acetabulum forms a cup within which the femoral head is partly contained. Its anterior and posterior rims

are clearly defined. Centrally located within acetabulum is fat surrounding the ligamentum teres[29].

The sciatic nerve, located directly posterior to the posterior column of the acetabulum, demonstrates intermediate signal intensity. It exits the pelvis through the greater sciatic foramen inferior to the piriformis muscle. Entrapment of the sciatic nerve at this location may be associated with the piriformis syndrome which is an asymptomatic hypertrophy of the piriformis muscle best appreciated on axial images. The piriformis divides the greater sciatic foramen into superior and inferior portions. The external iliac vessels, which are of low signal intensity, are medial to the iliopsoas muscle and anterior to the anterior acetabular column. The low signal intensity tendon of the rectus femoris blends with the low signal intensity cortex of the anterior inferior iliac spine. The tendon of the reflected head of the rectus femoris muscle is anterolateral to the iliofemoral ligament and follows the contours of the lateral acetabulum [29].

At the level of the femoral head (fig.11), the more distal femoral artery and vein are visualized. The femoral head articular cartilage demonstrates intermediate signal intensity, and the anterior and

posterior fibrocartilaginous acetabular labrum may also be identified, acetabular labrum is triangular, with the apex oriented laterally at this level [29].

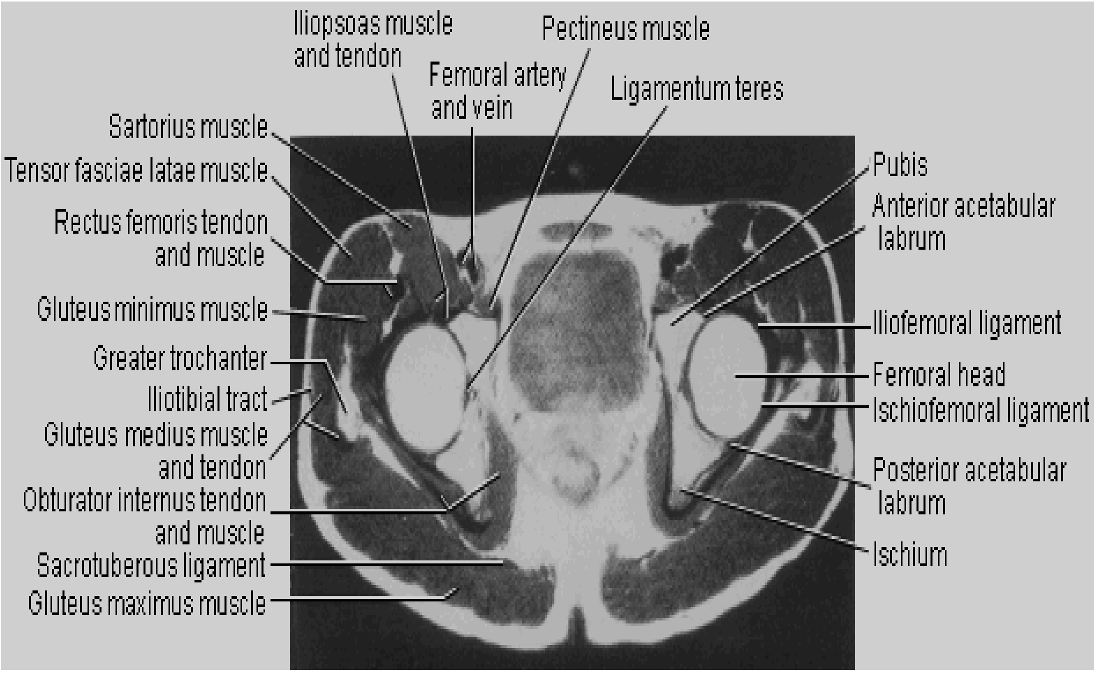

Figure (11): MR axial T1WI at the level of the femoral head[29].

<u>At the level of the greater trochanter and femoral neck</u> (fig.12), the obturator internus is identified medial to the pubis and ischium. The iliofemoral ligament is of low signal intensity and blends with the low signal intensity cortex of the anterior femoral neck. The sciatic nerve, lateral to the ischial tuberosity, is encased in fat between the quadratus femoris muscle anteriorly and the gluteus maximus

muscle posteriorly(29).

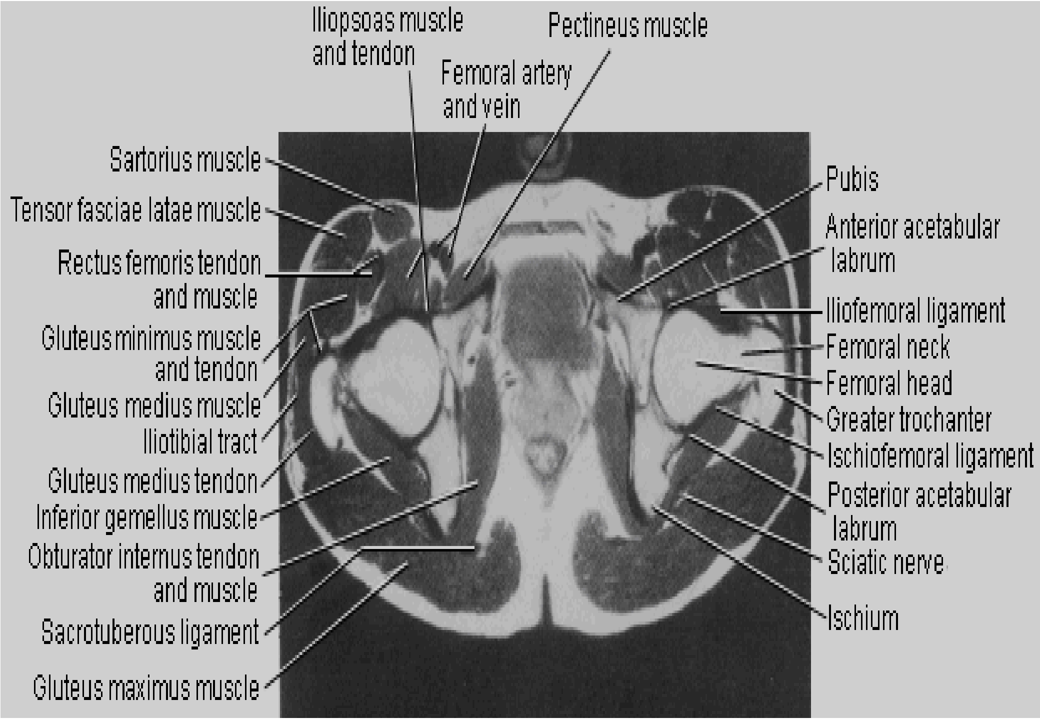

Figure (12): MR Axial T1WI at the level of the greater trochanter(29).

The iliotibial tract can be seen peripherally as a thin, low signal intensity band surrounded by high signal intensity fat on the medial and lateral surfaces. The low signal intensity obturator vessels are encased in high signal intensity fat and can be identified posterolateral to the pubic bone. The ischiofemoral ligament is also identified medial to the ischium, and applied to the posterior hip capsule. The sacrotuberous ligament is seen posteromedial to the ischium (29).

Sagittal Images:

<u>On lateral sagittal images,</u> the ilium, the anterior inferior iliac spine, the acetabular roof, and the femoral head are seen on the same sagittal section. The gluteus medius muscle and the tendon attachment to the greater trochanter are demonstrated on lateral sagittal images. The tendon of the obturator externus is anterior and inferior to the greater trochanter. The piriformis tendon is situated between the iliofemoral ligament anteriorly and the gluteus medius tendon posteriorly (fig.13). The iliofemoral ligament extends inferiorly, directly anterior to the anterior acetabular labrum. The iliopsoas muscle and tendon course obliquely anterior to the iliofemoral ligament, anterior to the femoral head. The ischiofemoral ligament is closely applied to the surface of the posterior femoral head. The femoral physeal scar is seen as a horizontal band of low signal intensity, in an anterior to posterior orientation [29].

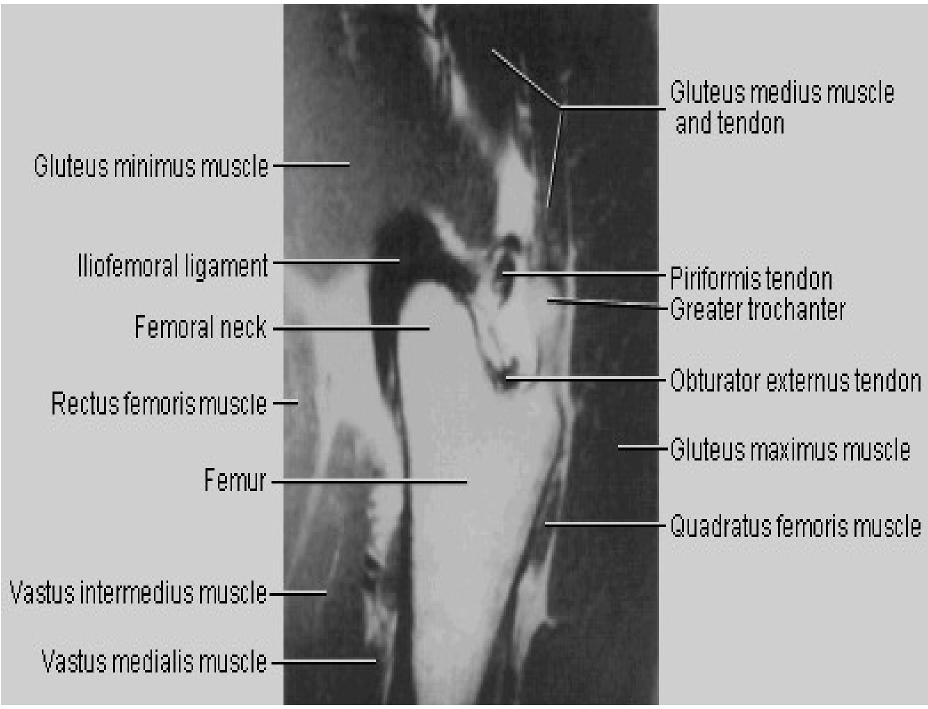

Figure (13): MR lateral sagittal T1WI[29].

In the mid sagittal plane (fig. 14), the intermediate signal intensity hyaline cartilage of the femoral head and acetabulum can be separately defined, and the posterior gluteal and anterior rectus femoris muscles are displayed in the long axis. The sciatic nerve can be followed longitudinally between the anterior quadratus femoris and the posterior gluteus maximus. The low signal intensity attachment of the sartorius to the anterosuperior iliac spine is shown anteriorly on Sagittal images. The low signal intensity iliopsoas tendon spans the hip joint anteriorly, crossing to its insertion on the lesser trochanter, The adductor

muscle group is displayed inferior to and medial to the iliopsoas tendon and the pectineus muscle[29].

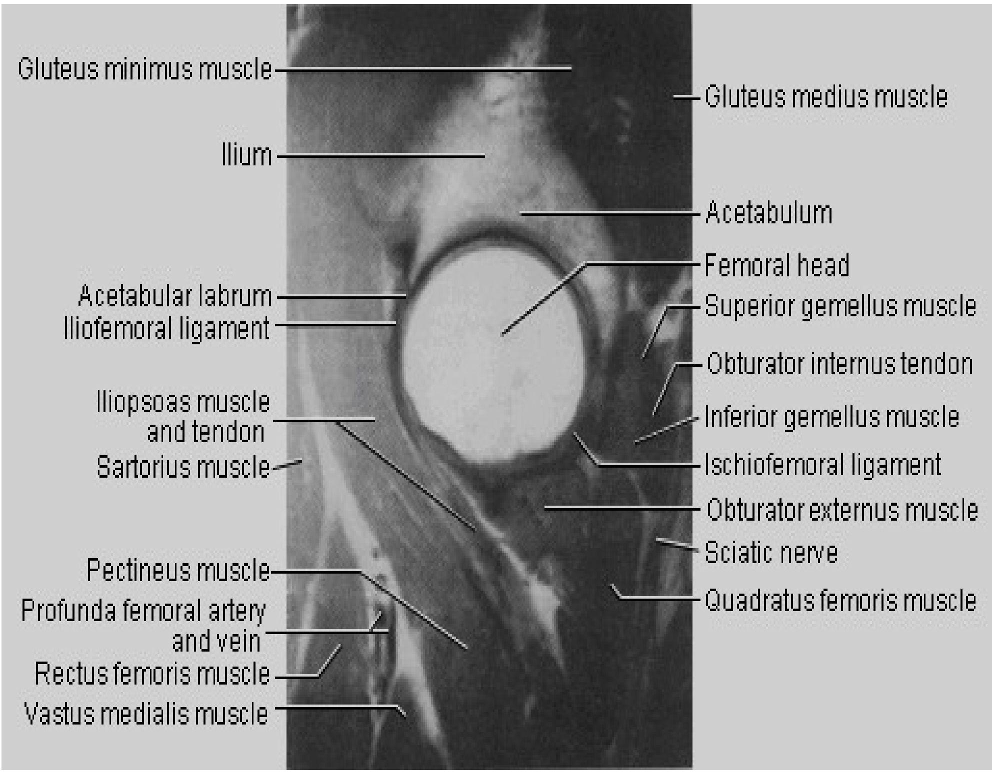

Figure (14): MR mid sagittal T1WI[29].

<u>On medial sagittal images</u> (fig.15), the acetabulum encompasses 75% of the femoral head, and the low signal intensity transverse acetabular ligament bridges the uncovered anterior inferior gap. On extreme medial images through the hip joint, the ligamentum teres may be seen within the acetabular fossa. At this level, the ischial tuberosity can be seen posterior and inferior to the acetabular fossa [29].

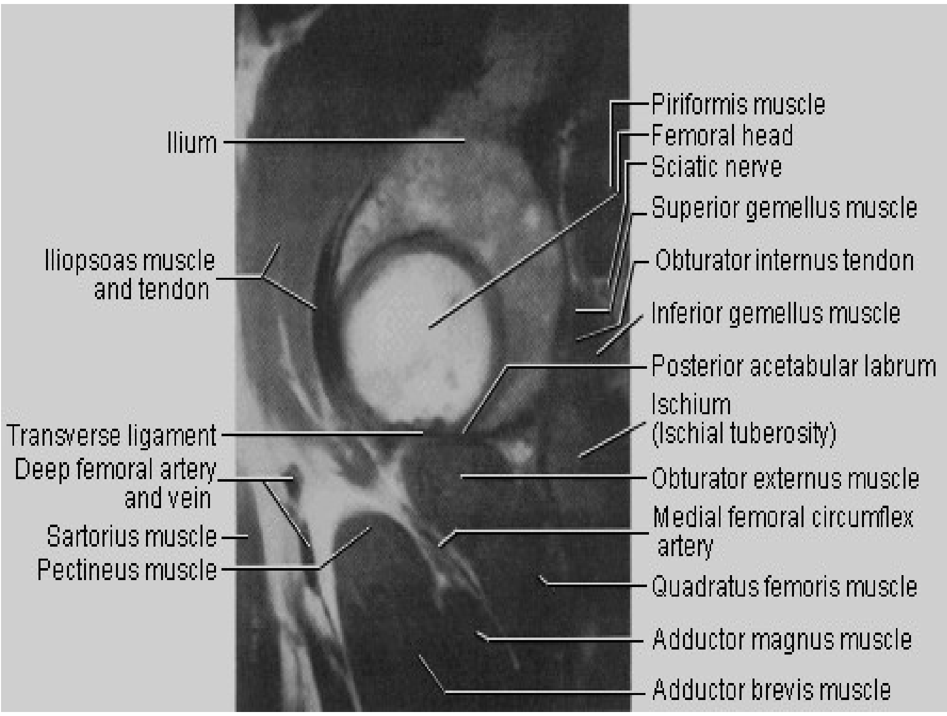

Figure (15): MR medial sagittal T1WI[29].

Coronal Images:

The coronal plane is used in the evaluation of the acetabular labrum, the hip joint space, and the subchondral acetabular and femoral marrow, as seen on coronal gross and MRI sections. Acetabular and femoral head articular cartilage may be more difficult to separate on coronal images than on sagittal images. The acetabular labrum, is visualized as a low signal intensity triangle interposed between the superolateral aspect of the femoral head and the inferolateral aspect of the acetabulum. The joint capsule is visualized as a

low signal intensity structure circumscribing the femoral neck. In the presence of fluid, the capsule distends and the lateral and medial margins become convex. Anterior coronal images (fig.16) demonstrate that the articular cartilage of the femoral head can be seen medially at the ligamentum teres insertion site. The reflected head of the rectus femoris is shown lateral to the proximal portion of the iliofemoral ligament [29].

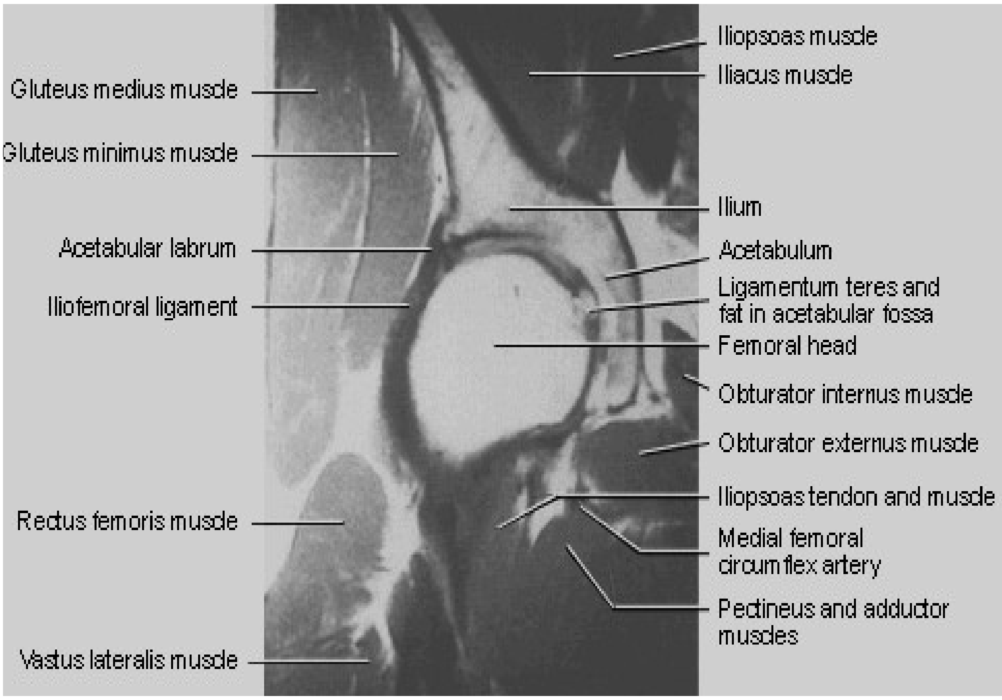

Figure (16): MR T1WI anterior coronal image[29].

The low signal intensity iliofemoral ligament is present on the lateral aspect of the femoral neck, near the greater trochanter. The superior acetabular labrum

is located deep to the proximal portion of the iliofemoral ligament along the lateral inferior margin of the acetabulum. The orbicular zone may be identified as a small outpouching on the medial aspect of the junction of the femoral head and neck. The intraarticular femoral fat pad is located between the medial femoral head and the acetabulum, and displays increased signal intensity on Tl-weighted images. In homogeneity of marrow signal intensity in the acetabulum, ilium, and ischium is a normal finding on Tl- weighted images. This represents normal red and yellow marrow in homogeneity (fig.17) [29].

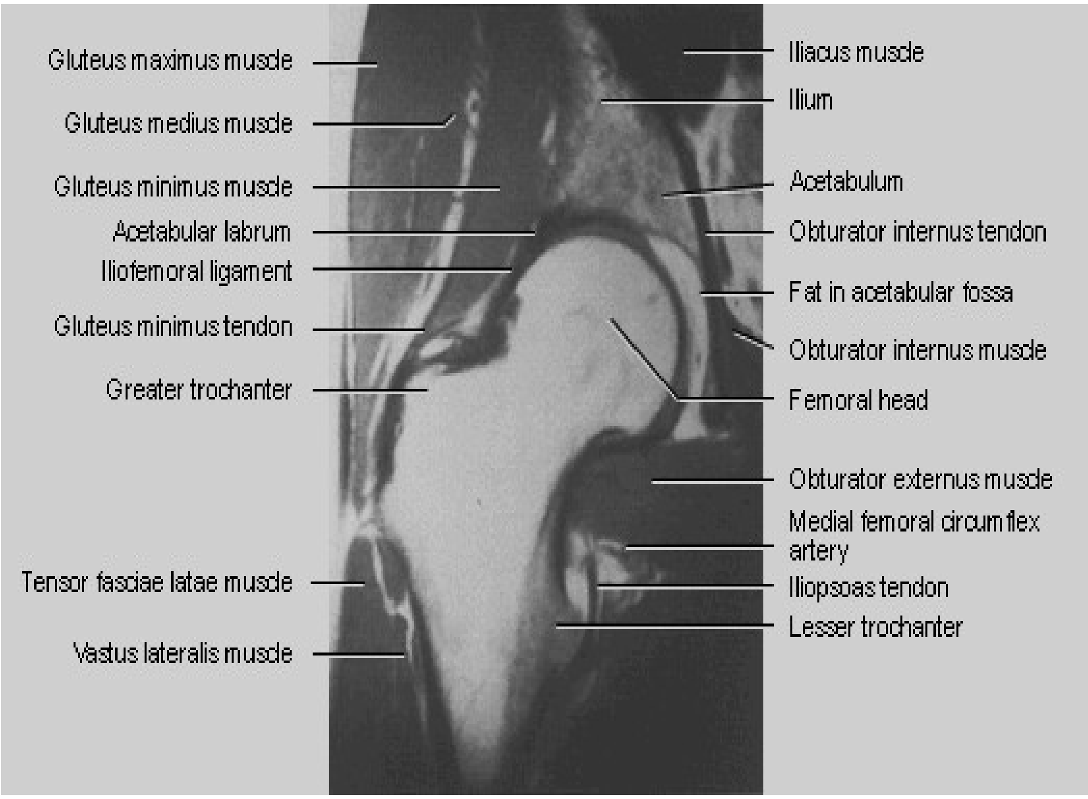

Figure (17): MR T1WI mid coronal image[29].

Normal signal pattern of the femoral head at different ages:

The lipid component of marrow provides a useful marker for marrow evaluation with MRI imaging. The predominance of fat content seen in yellow marrow results in high signal intensity on Tl weighted images and intermediate signal intensity on T2 weighted images. Hematopoietic marrow, with its lower fat content and higher water content, has intermediate signal intensity on both Tl and T2 weighted images. The

high signal intensity of fat may mask underlying processes, techniques that negate the fat signal intensity can be useful in evaluating subtle abnormalities[30].

The trabecular and cortical bone yield very little signal and are hypointense on MRI images obtained with all sequences. At birth, all the marrow produces blood cells, but by age 1 year, marrow in the epiphyses and apophyses is changed to inactive. As aging continues, the marrow continues to convert to yellow marrow but at a slower rate. Conversion of marrow in the femur begins in the diaphyses and progresses toward the metaphyses. Conversion of the marrow in the flat bones of the pelvis lags behind that in the lower extremity[31].

In the pelvis hematopoietic marrow is diffusely distributed, with areas of focal fatty marrow found around the sacroiliac joints, acetabula and symphysis pubis. This hematopoitic marrow may become more prominent or may be replaced by fatty marrow as patient age's .These changes tend to be bilateral and symmetrical[30].

CLINICO -PATHOLOGICAL ASPECT OF NON TUMORAL FEMORAL HEAD LESIONS

A . Avascular necrosis(Osteonecrosis):

Osteonecrosis is a disease arising from impaired osseous blood flow which can follow traumatic or non-traumatic conditions. Originally it was thought to be secondary to infection, but negative bacteriological studies led to the use of the term aseptic necrosis. Further studies showed that the necrotic bone was not only sterile but also avascular, hence the terms ischaemic necrosis, avascular necrosis, and bone infarction[32].

Avascular necrosis (AVN) is defined as cellular death of bone components due to interruption of the blood supply ;the bone structures then collapse, resulting in bone destruction, pain, and loss of joint function. Early diagnosis and appropriate intervention can delay the need for joint replacement. However, most patients present late in the disease course. Without treatment, the process is almost always progressive, leading to joint destruction within 5 years[33].

Osteonecrosis of the femoral head may lead to progressive destruction of the hip joint. Although the etiology of osteonecrosis has not been definitely delineated, risk factors include corticosteroid use, alcohol consumption, trauma, and coagulation abnormalities. Size and location of the lesion are prognostic factors for disease progression and are best assessed by MRI[34].

Sequelae of avascular necrosis

***Minimal disease*: ** If the vascular area is small and not

adjacent to an articular surface, the patient may be asymptomatic and may heal spontaneously, and the disease may remain undetected or be discovered incidentally during workup for other conditions[35].

***More severe disease*:** Once AVN develops, repair begins at the interface between viable and necrotic bone. Ineffective resorption of dead bone within the necrotic focus is the rule. Dead bone is reabsorbed only partially. Reactive and reparative bone is laid down on dead trabeculae resulting in a sclerotic margin of thickened trabeculae within an advancing front of hyperemia, inflammation, bone resorption, and fibrosis. The incomplete resorption of dead bone results in a mixed sclerotic and cystic appearance on radiographs. Necrosis and repair are ongoing in various stages of evolution within a single lesion[35].

Mechanical failure: Mechanical failure of trabecular bone at the interface between dead and viable bone may exacerbate AVN. In the subchondral region, such microfractures do not heal because they occur within an area of dead bone. Progression of the microfractures results in a diffuse subchondral fracture, seen radiographically as the crescent sign. Following subchondral fracture and progressive weightbearing, collapse of the articular cartilage occurs. Continued fracture, necrosis, and further weight bearing can progress to degenerative joint disease (DJD) and joint dissolution[36].

Causes of avascular necrosis[37].

A: Traumatic causes

B: Non Traumatic causes as

- Legg-Calvé-Perthes (LCP) disease.
- Alcoholism.
- Cortico-steroid excess.
- Decompression sickness (Caisson disease).
- Metastatic disease.
- Pancreatic disease.
- Hemoglobinopathies, hemophilia, sickle cell disease and thalassemia.
- Hypercoagulable states.
- Irradiation.
- Gaucher disease.
- Pregnancy.

Trauma:

Trauma is the most common cause of AVN. It can occur within 8 hours after traumatic disruption of the blood supply. The superior retinacular vessels and the nutrient artery can be damaged as they enter the femur. The artery of the ligamentum teres (ALT) also may be damaged. Intracapsular hematoma increases intracapsular pressure, which can cause tamponade of the vessels within the joint capsule. Intertrochanteric and extracapsular fractures of the femur rarely develop AVN. Following hip dislocation, circulation is interrupted because of tears of the ligamentum teres, tearing the ALT. Tearing of the joint capsule compromises the vessels within the capsular reflections[38].

The classic mechanism of injury for femoral head fracture is traumatic posterior dislocation of the hip. Shear forces against the femoral head as it exits from the acetabulum are thought to cause the femoral head fracture during hip dislocation. Due to the inherent stability of the hip joint, dislocation of the hip with associated femoral head fracture requires high amounts of energy, most often due to motor vehicle collisions, fall from a height, motor vehicle-pedestrian accidents, and sports injuries[(39)].

The Pipkin classification is the most widely used classification system(Fig. 18), which is based on the location of the femoral head fracture in relation to the femoral head fovea and the present of any associated fractures. Type I femoral head fractures occur when the fracture is inferior to the fovea centralis, whereas type II femoral head fractures extend superior to the fovea centralis. Type III is any femoral head fracture that is associated with a concomitant femoral neck fracture, and a type IV is associated with an acetabular fracture[(39)].

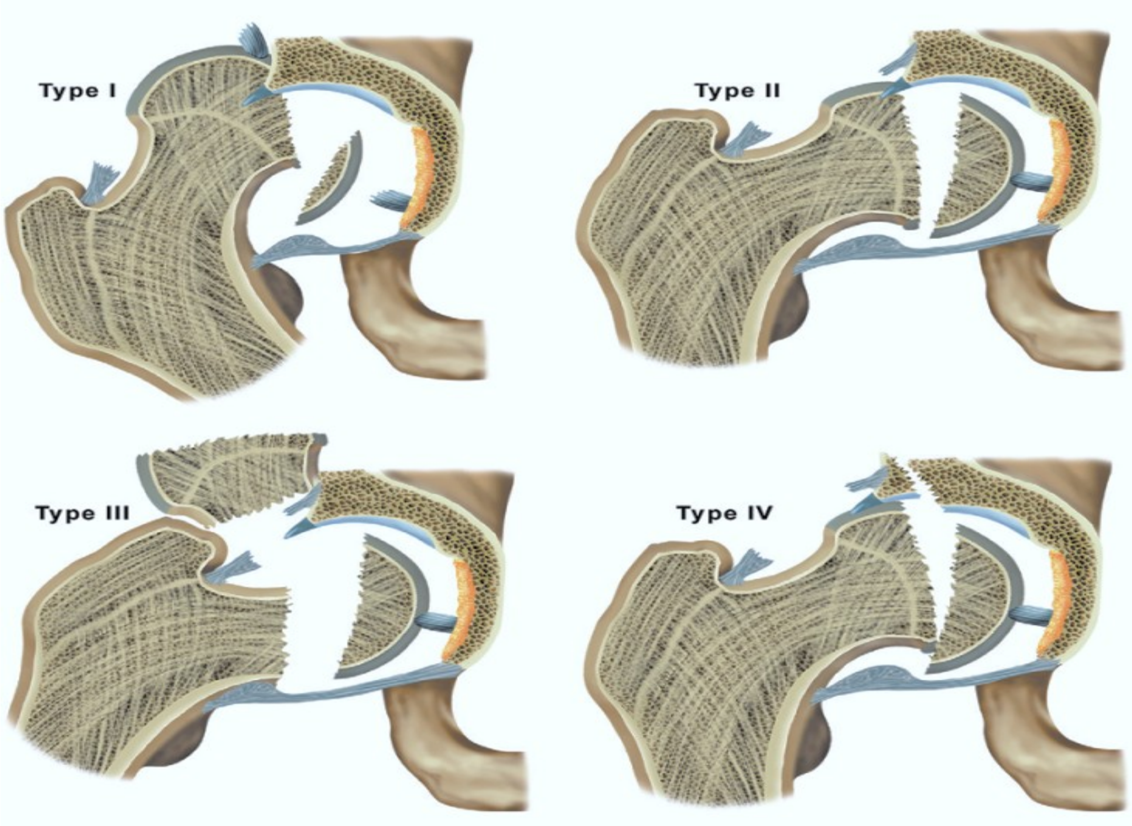

Figure (18): Pipkin classification of posterior hip dislocations[40].

Slipped capital femoral epiphysis(SCFE) is the most common hip disorder in adolescents, and it has a prevalence of 10.8 cases per 100,000 children. It usually occurs in children eight to 15 years of age, and it is one of the most commonly missed diagnoses in children. Slipped capital femoral epiphysis is classified as stable or unstable based on the stability of the epiphyseal plate. The condition is associated with obesity and it is occasionally associated with endocrine disorders such as hypothyroidism, growth hormone supplementation, hypogonadism, and panhypopituitarism. Patients usually present with limping and poorly localized pain in the hip, groin, thigh, or knee[41].

Classification of SCFE is based on the stability of the epiphysis. If the patient is able to move with or without crutches, the SCFE is considered stable. If the patient is unable to move

even with crutches, the SCFE is considered unstable. Stable SCFE accounts for about 90 percent of all slips. Classification is important because a stable SCFE generally has a better prognosis than an unstable SCFE, which has a higher rate of complications[41].

Sequelae of slipped capital femoral epiphysis include severe varus deformity, shortening and broadening of the femoral neck, osteonecrosis, chondrolysis, and degenerative joint disease[42].

Legg-Calvé-Perthes (LCP) disease:

Perthes disease remains one of the most controversial topics in all of pediatric orthopaedic surgery. The debate about its etiology and pathogenesis continues, and there is also debate regarding treatment. It is a disorder of the hip in young children. The condition was described independently in 1910 by Legg, Calve and Perthes'[43].

It is more common in boys than in girls by a ratio of 4 or 5 to 1. The incidence of bilaterality has been reported as 10% to 12%. Although the incidence of a positive family history in patients with Legg- Calve-Perthes syndrome ranges from 1.6% to 20%, there is currently no evidence that this syndrome is an inherited condition[43].

Legg-Calvé-Perthes disease is the most common cause of AVN in children. it's time of onset ranges from age 3-10 years . The vascular anatomy of the proximal femur is in a transitional stage of development in children aged 4-7 years, making the blood supply to the femoral head especially susceptible to injury. The artery of the ligamentum teres does not penetrate the epiphysis of the

femoral head until age 9 or 10 years. The epiphyseal growth plate prevents communication between the blood supply of the epiphysis and metaphysis, thus the femoral head is at increased risk for developing AVN, even from minor trauma[44].

Patients with Legg-Calve-Perthes syndrome most commonly present with a history of gradual onset of limping. Most patients do not complain of much discomfort, unless specifically questioned about this aspect[45].

Pain, when present, is usually activity-related and relieved by rest. Because of the mild nature of the symptoms, most patients do not present for medical attention until weeks or months after the clinical onset of disease[45].

The pain is generally localized to the groin, or referred to the anteromedial thigh or knee region. Failure to recognize that the thigh or knee pain in the child may be secondary to hip pathology may cause further delay in the diagnosis. Some children present with more acute onset of symptoms. Seventeen percent of patients with Legg-Calve- Perthes disease may have a history of related trauma[46].

Alcoholism:

Alcohol may have a toxic effect on osteogenic cells. The direct toxic effect of alcohol results in fat deposition in the liver. Livers with fat deposits are a constant source of low-grade asymptomatic fat emboli. Intraosseous fat emboli become hydrolyzed to free fatty acids, which cause endothelial damage. Alcohol intake exceeding 40 ml per week increases the risk of AVN more than 11 times compared to the risk in nondrinkers[47].

Cortico-steroid excess:

Both endogenous (cushing's syndrome) and exogenous cortico- steroid excess are associated with osteonecrosis .the risk of AVN is greater risk in patients treated for a short duration with high doses. However, the risk of AVN in low-dose steroid therapy is controversial(48).

Metastatic disease:

Metastatic cells can infiltrate the marrow, resulting in increased intramedullary pressure obstructing the intramedullary vessels. Patients are at higher risk if they are receiving steroid therapy and/or are undergoing local radiation therapy to the hip(49).

Pancreatic disease:

The release of lipolytic enzymes into the bloodstream results in breakdown of the fat within the marrow cells into free fatty acids, which are toxic to endothelium, causing intravascular coagulation. Upon entering the portal venous radicals in patients with pancreatitis, pancreatic enzymes can cause release of intracellular fat from fat- laden hepatic cells(49) .

Hemoglobinopathies :

Infarcts in hemoglobinopathies tend to be large and occurs when a sickle gene is present to cause the sickling phenomena. Sickling of abnormal red blood cells occurs in intramedullary capillaries and venules, causing hyperviscosity and vascular occlusion. Bone marrow hyperplasia resulting from chronic anemia may pack the marrow, placing it at increased risk for developing AVN from elevated intramedullary pressure(50).

Irradiation:

Fibrosis and endothelial proliferation resulting from radiation induced arteritis cause underlying vascular compromise. Patients with metastatic lymphoma or carcinoma to the femoral head who are treated with steroids and chemotherapy are at increased risk of developing AVN. Depending on the dosage of radiation therapy, there may be a direct cytotoxic effect especially on the sensitive haematopoitic marrow(51).

B. Osteoarthritis (OA):

OA of the hip joint generally presents with fairly steady pain that becomes more severe as the disease advances. Progressively worsening pain with activity is common, and a painful, limping gait generally develops. Pain is worse initially with full internal rotation and extension of the hip, and hip range of motion is progressively lost(52).

Pathophysiology: Traditionally, OA has been considered a disease of articular cartilage. The current concept holds that OA involves the entire joint organ, including the subchondral bone and synovium. OA has always been classified as a non inflammatory arthritis. Cartilage is grossly affected. Focal ulcerations eventually lead to cartilage loss and Subchondral bone formation occurs as well, with development of bony osteophytes(53).

Hip osteoarthritis was classified into categories ranging from early- to terminal- stage disease on the basis of radiological observations. The early stage was characterized by a slight narrowing of the joint space; this was associated with sclerosis of

the subchondral bone. The advanced stage was characterized by an obvious narrowing of the joint space, with some cystic changes and the presence of small osteophytes in the femoral head and/or the acetabulum. The terminal stage was characterized by the disappearance of the joint space with marked osteophyte exposure(54).

OA of the hip may lead to migration of the femoral head superiorly (78%) or medially (22%). The acetabulum may be deepened following medial migration or show new bone medially and superolaterally following lateral migration of the femoral head. Capsular traction leads to new bone formation, usually on the medial rather than the lateral aspect of the femoral neck(52).

C. Inflammatory Arthritis:

Pain is also a presenting complaint in much inflammatory arthritis, including(55):

1. Seropositive arthritis (rheumatoid).
2. Seronegative spondyloarthropathies (ankylosing spondylitis, systemic lupus erythematosus, Reiter's syndrome, psoriatic arthropathy & enteropathies arthropathy).
3. Crystalline arthropathies (Gout and pseudo gout).
4. Infective (viral and septic arthritis).

Although the course of the inflammatory arthritis is unknown, the underlying pathology is that of inflammation. Early, the synovial tissue is hyperaemic and oedematous leading to secretion of large amounts of protein rich synovial fluid into the joint.

Continued inflammation leads to synovial hypertrophy. Collapse, narrowing of the joint space, avascular necrosis, fibrous ankylosis and bony fusion may finally occur[(53)].

Rheumatoid Arthritis (RA): RA of the hip is usually a late manifestation of more widespread disease. RA is associated with soft tissue swelling which is due to edema of periarticular tissues and to synovial inflammation in bursae, joint spaces and along tendon sheathes. Joint distension also follows an increase in synovial fluid. Local osteoporosis around joints occurs early and is due to synovial inflammation and hyperemia[(55)].

Ankylosing Spondylitis: The osteoporosis, erosions and joint space narrowing are less prominent than in rheumatoid arthritis, but periostitis and ankylosis are more common[(53)].

Systemic Lupus Erythematosus: It is a systemic connective disorder, occurs mainly in young females and may be difficult to differentiate from RA. Although joint pain is usual, it is often over shadowed by systemic illness. A painful, debilitating red, hot arthritis may occur due to vasculitis, affecting any joint, with marked restriction of its movements[(56)].

Septic Arthritis: Acute purulent infection of the joints is more common in infancy and early childhood due to the greater blood flow to the joints during the active stages of growth. The usual cause is hematogenous dissemination related to an upper respiratory infection or pyoderma. Infection may also spread from adjacent osteomyelitis, cellulitis, abscess, or traumatic joint invasion. In children, septic arthritis develops commonly from osteomyelitis in metaphyses that are intraarticular, such as the hip.

The diagnosis of the obvious septic joint is not much of a challenge, although time to diagnosis is critical to avoid a poor outcome such as destruction of the femoral head, degenerative arthritis, or permanent deformity(57).

In septic arthritis, bacterial contamination causes hypertrophy and edema of the synovium. In infants with septic arthritis, distension of the joint capsule may result in pathologic dislocation particularly in the hip. Joint space narrowing results from cartilage destruction by proteolytic enzymes. There may be associated bone erosion and destruction or periosteal reaction. Pus in the joint increases intraarticular pressure and may result in osteonecrosis of the epiphysis(57).

D. Idiopathic Transient Osteoporosis of the Hip (ITOH):

Transient osteoporosis of the hip(TOH) is an uncommon cause of hip pain. It affects mostly healthy middle-aged men, and women in the third trimester of pregnancy. It is self-limiting and resolves symptomatically and radiologically within some months of presentation. The aetiology is unknown. In 25% of reported cases no cause was found. In the remainder, trauma, either minor or major, had occurred in half. Other suggested triggering factors are neuralgia, herpes zoster, hemiplegia and vascular disturbances. It has been proposed that TOH is a form of reflex sympathetic dystrophy because of its diffuse pattern around the affected joint and the migratory involvement of other joints(58).

Predisposing factors include compromised blood flow to the bone, hypercoagulable states, metabolic and endocrinologic disturbances, orthopedic problems, dietary or environmental

factors, and iatrogenic causes[59].

E. Developmental dysplasia of the hip

Developmental dysplasia of the hip refers to a number of abnormalities in the immature hip that can range from subtle dysplasia to dislocation. The identification of risk factors, including breech presentation and family history, should raise a physician's suspicion of developmental dysplasia of the hip. Diagnosis is made by physical examination. Palpable hip instability, unequal leg lengths, and asymmetric thigh skinfolds may be present in newborns with a hip dislocation, whereas gait abnormalities and limited hip abduction are more common in older children[60].

Hip dysplasia refers to an abnormality in the size, shape, orientation, or organization of the femoral head, acetabulum, or both[60].

The origin and pathogenesis of DDH are multifactorial. Abnormal laxity of the ligaments and hip capsule is seen in patients with DDH. The maternal hormone relaxin may also be a factor. Oligohydramnios and being a first-born child also may have a role. Extreme hip flexion with knee extension, as in the breech position, tends to promote femoral head dislocation and leads to the shortening and contracture of the iliopsoas muscle[61].

MR EXAMINATION PROTOCOLS &IMAGING TECHNIQUES OF THE HIP JOINT

MRI provides a uniquely comprehensive assessment of bone and soft-tissue abnormalities in patients with hip pain, identifying the anatomic site and tissue complexity of the pathology. Recognition of abnormal signal intensity patterns involving bone and soft-tissue promotes accurate diagnosis of osteonecrosis, stress injury, acute traumatic injury, neoplasm, and arthropathy[(62)].

Although there is no ionizing radiation with MRI and thus no biological hazards have been identified. There are certain practical considerations must be taken in order to obtain a good MR image[(63)].

These considerations include [(63)]**:**

1) Claustrophobia: Despite the small incidence of claustrophobia among patients undergoing MR imaging, it is a potential problem that sometimes requires oral sedation.

2) The patient's clinical status must be considered. Magnetic resonance examinations may require 13-60 min. This necessitates making the patient comfortable so that he remains stationary for fairly long period of time. Patient with significant pain may require sedation or pain medications.

3) External fixation devices may be bulky and prohibit the use of surface coils.

Technique:

A-Patient Preparation[64]:

1. Have the patient go to the toilet before the study.
2. Explain the procedure to the patient.
3. Offer the patient ear protectors or ear plugs.
4. Have the patient undress except for underwear.
5. Ask the patient to remove anything containing metal (hearing aids, hairpins, body jewelry, etc.)

B-Positioning[64]:

1. Supine.
2. Body array coil (body coil, wraparound coil).
3. Cushion the legs with a small roll under the knees (do not elevate the thighs too much).
4. Have the patient cross the arms over the upper

abdomen.

C-Coil selection :

In MR imaging, every attempt should be made to use the smallest coil possible to produce the maximum signal. One factor that must be considered when selecting a coil relates to its size. It must be able to detect signal from the entire length and depth of the tissues of interest[63].

D-Image orientation :

The most useful information for evaluating hip pathology can be obtained in the axial and coronal planes. Sagittal images sometimes can be difficult to interpret because the fovea centralis may mimic pathology, and these images generally give no additional information[63].

- Suggested parameters using a 1.5-T magnet[65]:
  - Pelvic or torso phased-array coil.
  - Slice thickness: 3 to 4 mm.
  - Matrix: 512 × 512.
  - Field of view: 30 to 40 cm.

Axial sections from the top of the iliac crest to below the lesser trochanters. Coronal sections from the sacroiliac joint to the pubic symphysis. Sagittal sections from the anterior acetabulum to the posterior acetabulum . Oblique sagittal sections following femoral neck orientation[65] (Fig. 19)(table 2).

- Gadolinium injection may be necessary to assess femoral head vascularization, suspected infection, or bone or soft tissue

tumors. Always compare with the unaffected side. To depict Legg-Calvé-Perthes disease the use of dynamic technique is recommended[65].

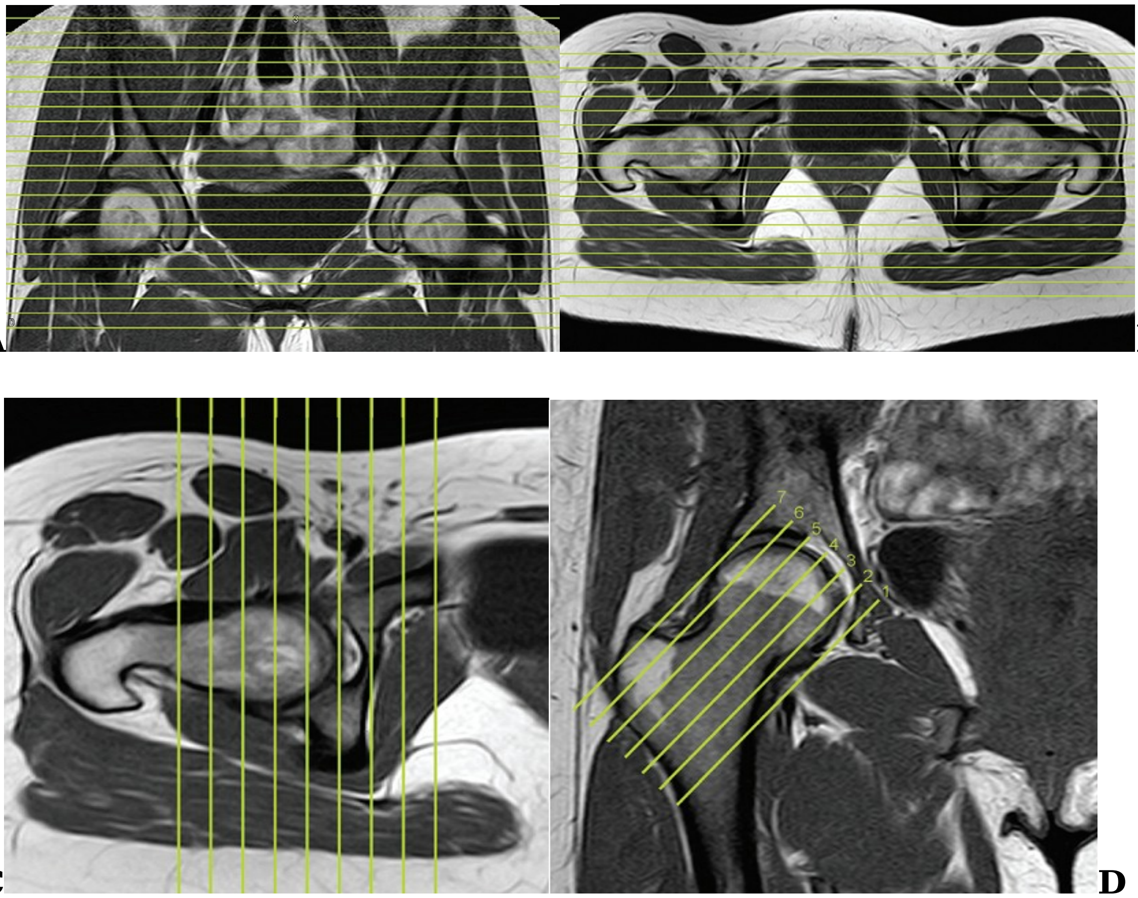

Figure 19 : Pelvis MRI, A: Coronal image shows axial sections from the top of the iliac crest to below the lesser trochanters. B:Axial image shows coronal sections from the sacroiliac joint to the pubic symphysis. C: Axial image shows sagittal sections from the anterior acetabulum to the posterior acetabulum. D: Coronal image shows oblique sagittal sections follow femoral neck orientation[65].

Table(2):Features of conventional pelvic magnetic resonance imaging of the hip-pelvis[65].

Imaging Planes	Pulse Sequences
Axial	T1-weighted, fast spin-echo, proton density–weighted; T2-weighted fat saturated; STIR
Coronal	T1-weighted, fast spin-echo, proton density–weighted; T2-weighted fat saturated
Sagittal	T1-weighted; fast spin-echo T2-weighted
Additional Optional	
Oblique sagittal	T1-weighted, STIR
Axial	Gradient-recalled echo

STIR, short tau inversion recovery.

Hip structures to evaluate in coronal plane[66]:

- Osseous structures:
  - Acetabulum.
  - Femoral head, neck.
  - Greater, lesser trochanter.
  - Sacrum.
  - Ilium.
  - Sacroiliac joints.
- Muscles:
  - Gluteal muscles.
  - Adductors.
  - Abductors.
  - Hamstrings.
  - Quadriceps.
- Labrum.

Hip structures to evaluate in axial plane[64]:

- Osseous structures:
  - Acetabulum.
  - Femoral head, neck.
  - Greater, lesser trochanter.
  - Sacrum.
  - Ilium.
  - Sacroiliac joints.
- Muscles:
  - Gluteus maximus, medius, and minimus.
  - Sartorius, rectus femoris.
  - Gracilis, pectineus, adductor longus, brevis, and magnus.
  - Tensor fascia lata.
  - Piriformis.
  - Obturator internus, externus.
  - Gemelli superior and inferior.
  - Quadratus femoris.
- Labrum.

E- Pulse sequences :

The main stem of musculoskeletal MR imaging is the spin-echo sequence, including T1-weighted, T2-weighted, and proton-density (PD)-weighted images(Table 3). The relative contrast of the image will vary depending on the parameters of the particular imaging system(67).

Table 3: Pulse sequences: Imaging parameters (or "how to recognize a sequence by the numbers")[63]

Sequence	**TR (msec)**	**TE (msec)**	**TI (msec)**	**Flip Angle (º)**	**ETL**
T1	< 1000	< 30	N/A	90	N/A
Proton density	> 1000	< 30	N/A	90	N/A
T2	> 2000	> 60	N/A	90	N/A
FSE T2	> 2000	> 60	N/A	90	2-16
GRE T1	Variable	< 30	N/A	70-110	N/A
GRE T2*	Variable	< 30	N/A	5-20	N/A
FSE STIR	> 2000	> 60	120-150	180 -> 90	2-16

(ETL, echo train length; FSE, fast spin echo; GRE, gradient echo; N/A, not available; TE, echo time; TI, inversion time; TR, repetition time.)

1) Conventional Spin-Echo sequences:

Conventional spin echo pulse sequences include T1-weighted (T1W), T2-weighted (T2W), and proton density–weighted sequences:

T1-Weighted Spin Echo Sequence

TI-weighted spin echo images (T1-SE) (TR <800 msec; TE <30 msec) are obtained with a relatively short TR. The echo time TE is chosen to be as small as possible to minimize T2 signal decay, and keep a pure T1 contrast. As a result of the short TR,

structures with a long T1 relaxation time become progressively saturated and demonstrate low signal intensity (e.g. muscles and fluid-containing structures). Fat, however, which has a very short T1, demonstrates high signal intensity. T1-SE in the hip is used primarily for evaluation of bone marrow disorders such as avascular necrosis and detecting fractures or overuse syndromes[68].

T2-Weighted Spin Echo Sequence

T2-weighted spin echo images (T2-SE) (TR >2000 msec; TE >60 msec) are obtained with a relatively long TR to minimize T1 saturation effects. The echo time TE is chosen to show differences in the T2 relaxation times. This occurs at echo times of around 60–100 ms. At this TE all body fluids produce a high signal intensity due to its T2 relaxation characteristics. Muscle, however, is of relatively low signal intensity and fat is of intermediate signal intensity. The SNR in these images is inferior to the SNR in proton density-weighted images, but the pathology, which is characterized by an increased fluid content, is accentuated. T2-SE are rarely used in evaluation of the hip because of the advantages of fast (turbo) spin echo T2 weighted images[68].

Proton Density-Weighted Spin Echo Images

Proton density-weighted spin echo images (PDSE) (TR >1000 msec; TE <30 msec) are obtained with a long TR and short TE and provide signal which reflects the density of protons within the imaging field. The TR must be long enough to make sure that all tissues have sufficiently recovered during the TR interval. In general, the choice of the TR also depends on the field strength as

the T1 relaxation times tend to increase with higher field strengths. Similar to the T1-weighted sequences, the echo time TE is chosen to be as small as possible to minimize T2 signal decay. Because the T1 and T2 effects are minimized the PD-SE images have a high SNR and are useful for providing anatomical detail[(68)].

2) Fast Spin Echo: (also known as turbo spin echo)

This technique allows for much more rapid acquisition of images than does the conventional spin echo method. This technique has some drawbacks:

First, the signal intensity of fat remains quite bright on fast spin echo T2W images. Consequently, pathology in subcutaneous fat or marrow may be obscured on these images because of the similar signal intensity of fat and fluid. This problem can be overcome by combining this technique with fat saturation.

Second, the fast spin echo technique can result in blurring along tissue margins, specially, when images are acquired using long echo train lengths (> 4). Although it uses a longer echo train length to decrease imaging time, the associated increase in blurring may result in missing some types of pathology[(63)].

3) Gradient Echo:

The gradient echo (TR variable; TE <30 msec; flip angle = 10-80 degrees) Family of pulse sequences was originally developed to produce T2W images in less time than was possible with a conventional spin echo technique. This is achieved by reducing TR values and substituting gradient refocusing for the 180 refocusing radio-frequency pulse. To permit adequate signal, reduced flip angles are often used. Although fluid appears bright on both

gradient echo T2W images [designated T2*W] and spin echo T2W images. Ligaments and articular cartilage are particularly well demonstrated with gradient echo sequences, as are fibro-cartilaginous structures such as glenoid labrum[63].

Gradient echo imaging can be performed using a two dimensional technique (in which slices are obtained individually) or a three-dimensional "volume" technique [63].

Three-dimensional technique permits thinner sections and offers high S/N ratio than two-dimensional images with comparable voxel size[63].

One feature of gradient echo sequence is heightened sensitivity to susceptibility effects. This refers to artifactual signal loss at the interface between tissues of widely different magnetic properties, such as metal and soft tissue. This feature can be advantageous when searching for subtle areas of hemorrhage. These sequences are useful for detecting loose bodies & soft tissue gas because of susceptibility effects but its disadvantage is the limitation of the use of gradient echo sequences in patients with metallic implants following surgery[63].

4) Inversion Recovery (STIR):

Inversion Recovery Historically known as short time inversion recovery (STIR) imaging, inversion recovery (TR >2000 msec; TE >30 msec; TI = 120-150 msec) is a fat saturation technique that results in markedly decreased signal intensity from fat and notably increased signal from fluid and edema. As a result, inversion recovery is an extremely sensitive tool for detecting most types of soft tissue and marrow pathology[63].

This is a fat saturation technique that results in markedly decreased signal intensity from fat and strikingly increased signal from fluid and oedema. As a result, it is extremely sensitive tool for detecting most types of soft tissue and marrow pathology. On a practical note, fast spin echoSTIR imaging is, in many respects, equivalent to a fast spin echo T2W sequence with fat saturation [(63)].

Recent advances in hip joint MRI

Advances in MRI of articular cartilage of the hip joint

MRI has long been an important tool in the diagnosis and management of articular cartilage pathology, but detecting and interpreting early cartilaginous degeneration with this technology has been difficult. Biochemical-based MRI has been advocated to detect early cartilaginous degenerative changes and assess cartilage repair[(69)].

Techniques such as T2 mapping and delayed gadolinium-enhanced MRI of cartilage take advantage of changes in the complex biochemical composition of articular cartilage and may help detect morphologic cartilaginous changes earlier than does conventional MRI., their ability to assess the microstructure of articular cartilage may eventually enhance the diagnosis and management of osteoarthritis. Cartilage damage can be classified into 5 grades according to modified Outerbridge classification as described in (table 4) below[(70)].

(Table 4): Modified Outerbridge classification for cartilage damage [(70)].

	Grade	Macroscopy	MRI
	0	Normal cartilage	Normal cartilage
	1	Rough surface; chondral softening	Inhomogenous, high signal; surface intact
	2	Irregular surface defects; <50% of cartilage thickness	Superficial ulceration, fissuring, fibrillation; <50% of cartilage thickness
	3	Loss of >50% of cartilage thickness	ulceration, fissuring, fibrillation; > 50% of the depth of cartilage
	4	Cartilage loss	Full thickness chondral wear with exposure of subchondral bone

MRI APPEARANCE OF SPECIFIC FEMORAL HEAD LESIONS

MRI proved to be an excellent modality not only for the early diagnosis of osteonecrosis but also for the detection of infections as well as occult injuries, in and around the hip joint, with superior contrast resolution and without harmful radiation. MRI is the diagnostic modality of choice for most disorders of the hip where radiographic findings are inconclusive. With MRI one can stage the pathology to
prognosticate and influence therapeutic decisions(71).

A. Avascular Necrosis:

MRI has been proven to be the most accurate test to diagnose osteonecrosis. It is more accurate than other imaging modalities. Osteonecrosis most frequently involves the anterior medial superior quadrant of the femoral head with increasing size of the necrotic fragment of bone, the entire femoral head may be involved. The classic appearance of osteonecrosis of the femoral head is the presence of a curvilinear "reactive interface" between the necrotic bone proximally and viable bone distally (fig.20) (72).

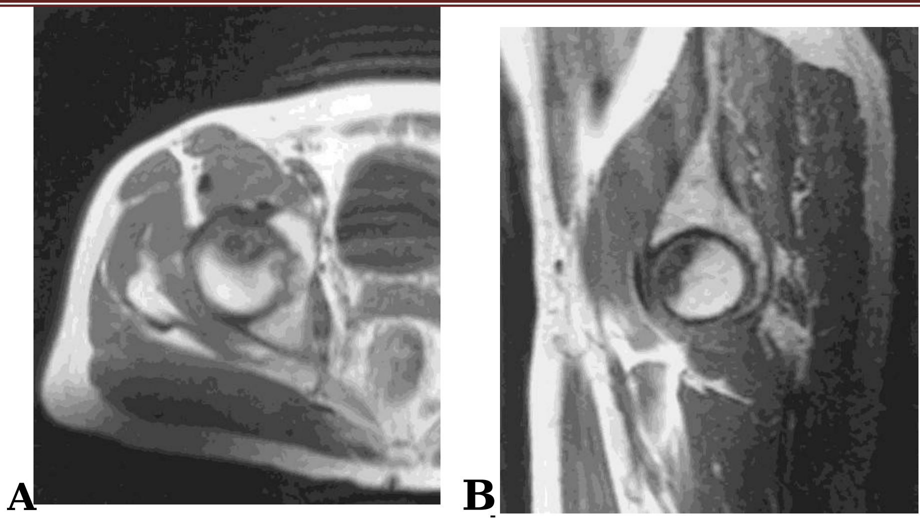

Figure (20): A. Axial T1-weighted image. The focal defect is located in the anterior portion of the femoral head. B. Sagittal T1-weighted image. The abnormal area is located in the anterosuperior portion of the femoral head[72].

T1 images on MRI typically demonstrate a serpiginous “band-like” lesion with low signal intensity in the anterosuperior femoral head, and a “double-line sign” can
be seen on T2 sequences, which depicts a high signal intensity reparative interface of vascular reactive bone adjacent to necrotic subchondral bone(fig.21) [73].

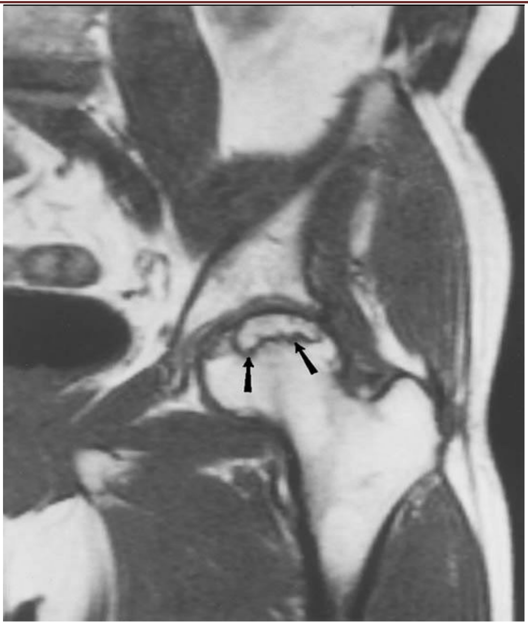

Figure (21): Coronal Tl-weighted image. A ring like low-signal line (arrows) surrounds an area of more normal signal within the femoral head [(73).]

When the trabeculae become coarse or collapse within the necrotic fragment, the necrotic bone becomes low signal intensity on both Tl and T2-weighted images. With more advanced osteonecrosis, a subchondral fracture may develop, which may appear as a hyper intense subchondral crescent on T2-weighted images. The presence of bone marrow edema is variable. The bone marrow edema is a potential cause for symptoms in early disease (fig.22) [(73)]

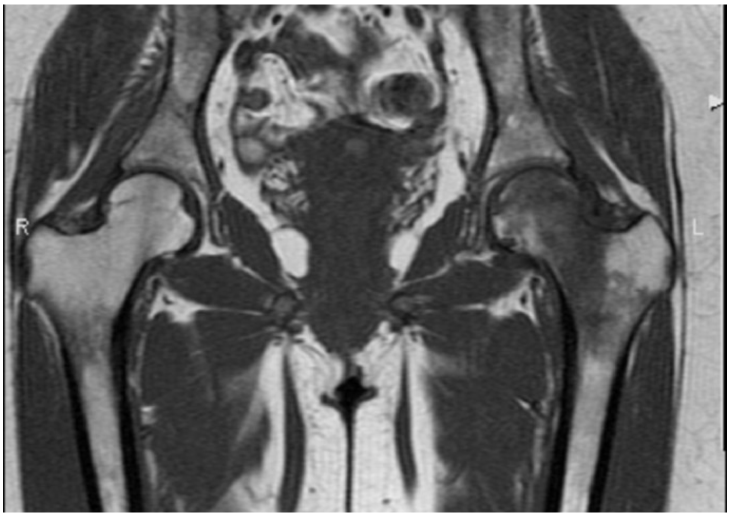

Figure (22): Initial T1-weighted imaging of the hips demonstrates the bone marrow edema pattern in the left hip (diffuse decreased signal) [73].

Recent attention has been drawn to the utility of MRI in predicting of early cases of osteonecrosis so will benefit from surgical intervention. The extent and location of the necrotic fragment on MR images is the best single predictor of the likelihood of collapse. To estimate the extent, the outline of the femoral head is best seen & estimated on the coronal images (table. 5) [74].

Table (5): The extent of the necrotic segment [74].

Grade A	Maximum radial distance from the circumference is
Grade	The distance is 1/4 to <1/2 of the
Grade	The distance is 1/2 the diameter or more.

One of the first classification systems utilized for this disease was that of Ficat and Arlet, who developed their system in the 1960s before the advent of magnetic resonance imaging depending on radiographic findings. This system has been modified at least four times. University of Pennsylvania proposed one of these modifications(table. 6). Their

important modifications included the incorporation of magnetic resonance imaging findings and the clear distinction into seven stages[75].

Table 6: Modified Ficat Staging System for Avascular Necrosis of the Hip[75].

STAGE	CRITERIA
0	**Normal or nondiagnostic radiograph, bone scan, and MRI**
I	**Normal radiograph; Abnormal bone scan and/or MRI** A – Mild (<15% of head affected) B – Moderate (15% to 30%) C – Severe (> 30%)
II	**Lucent and sclerotic changes in femoral head** A – Mild (< 15%) B – Moderate (15% to 30%) C – Severe (> 30%)
III	**Subchondral collapse (crescent sign) without flattening** A – Mild (<15% of articular surface) B – Moderate (15% to 30%) C – Severe (>30%)
IV	**Flattening of femoral head** A – Mild (<15% of surface and <2 mm depression) B – Moderate (15% to 30% of surface or 2 to 4 mm depression) C – Severe (>30% of surface or >4 mm depression)
V	**Joint narrowing and/or acetabular changes**

	A – Mild Average of femoral head involvement B – Moderate as determined in Stage IV, and C – Severe estimated acetabular involvement.
VI	**Advanced degenerative changes**

Stage 0 is both preclinical and preradiographic. Stage I demonstrates normal radiographic findings with abnormal findings on magnetic resonance images. Stage II shows diffuse or localized areas of sclerosis and/or lucencies in the femoral head. Stage III is characterized by the crescent sign (subchondral fracture). Stage IV demonstrates collapse and fracture involving the articular surface along with segmental flattening of the femoral head but no acetabular involvement. Stage V is characterized by the development of osteoarthritis showing acetabular changes in addition to the collapse of the femoral head, and Stage VI is defined by advanced degenerative changes of the joint(75).

The ARCO (Association Research Circulation Osseous) classification(table 7) has become increasingly popular in Europe in recent years. Besides staging bony changes, the ARCO classification also takes into account the extent and location of necrosis based on various imaging modalities (radiography, CT. magnetic resonance imaging [MRI], and scintigraphy)(76):

• ARCO stage 0 (initial stage): All imaging studies at this stage are negative. In theory, histology would show evidence of necrosis(76).

• ARCO stage 1 (reversible early stage): MRI and scintigraphy are already positive at this stage, whereas conventional radiographs still normal. Stage 1 is divided into three

subcategories according to the location and extent of necrosis. The location is classified as medial (A), central (B), or lateral (C) and is designated by the corresponding letter. The extent of necrosis is quantified by estimating the percentage involvement of the femoral head, and this is indicated by a second letter:< 15% (A), 15-30% (B), and > 30% (C) [76].

- ARCO stage 2 (irreversible early' stage); This stage is characterized by an increasing demarcation of the necrotic area. A specific change is the "double line" sign on MRI which circumscribes the necrotic area (granulation tissue plus sclerotic bone bordering on healthy bone). The necrotic segment shows structural bone changes (sclerosis and osteolysis) on plain radiographs. In time the healthy bone forms a sclerotic margin. This stage is sub-classified using the same criteria as in stage 1[76].

- ARCO stage 3 (transitional stage): The hallmark of ARCO stage 3 is a radiographically visible fracture. Most cases initially show a subchondral fracture, which forms a crescent-shaped lucency ("crescent sign") on radiographs and CT scans. This stage is marked by progressive flattening or distortion of the femoral dome, which will eventually collapse. There is still no evidence of joint-space narrowing or acetabular involvement. ARCO stage 3 is sub-classified by the relative extent of the subchondral fracture line-< 15% (A), 15-30% (B), and> 30% (C)-or by the amount of flattening of the femoral dome: < 2 mm (A), 2-4 mm (B), and > 4 mm (C). As in stages 1 and 2, the location of the necrosis is

classified as medial (A), central (B), or lateral (C) [76].

• ARCO stage 4 (late stage): This stage is characterized by the development of secondary osteoarthritis .Joint space narrowing is visible on radiographs and MRI. The classic signs of osteoarthritis are also visible on the acetabular side of the joint. Sub-classification is no longer necessary in stage 4[76].

The main advantage of the ARCO classification is that it addresses and summarizes the factors that are relevant to therapeutic decision making[76].

Table7: Association Research Circulation Osseous (ARCO) stages of osteonecrosis[76].

Imaging modalities, subclassifications	Stage 0	Stage 1	Stage 2	Stage 3	Stage 4
Imaging					
X-rays	Normal	Normal	Sclerosis and osteolysis in necrotic segment; sclerotic margin	(Subchondral) fracture; flattening of femoral dome	Osteoarthritis
MRI	Normal	Demarcated necrotic segment	Necrosis with reactive margin; "double-line" sign	(Subchondral) fracture	Osteoarthritis
CT	Normal	Normal	Sclerosis and osteolysis in necrotic segment; sclerotic margin; "asterisk" sign	(Subchondral) fracture; deterioration of spherical head shape	Osteoarthritis
Scintigraphy	Normal	Diffuse or cold spot	"Cold in hot" pattern	"Hot in hot" pattern	Hot spot
Subclassifications					
Location of necrosis	None	 Type A	 Type B	 Type C	None
Quantitation of necrosis	None	Percentage area of femoral head involvement: • A < 15% • B 15–30% • C > 30%		Length of subchondral fracture: • A < 15% • B 15–30% • C > 30% Dome depression • A < 2 mm • B 2–4 mm • C > 4 mm	None

MRI is a valuable tool in the evaluation of ***Legg-Calvé-Perthes Disease*** that may be used to guide both nonsurgical and surgical management of the condition. This imaging technique can be used to document the presence of femoral head necrosis, accurately stage the disease process, provide important prognostic information, and diagnose a variety of associated complications. Contrast enhanced MRI may prove to be particularly beneficial in

the evaluation of suspected early (radiographically occult) proximal femoral epiphyseal necrosis and in the evaluation of femoral head revascularization[77].

Using a combination of unenhanced and contrast enhanced imaging sequences, this condition can be confidently diagnosed, even in the setting of normal or equivocal hip radiographs. Contrast enhanced imaging is particularly useful in the assessment of proximal femoral epiphyseal perfusion. Hypoperfusion of the proximal femoral epiphysis may be one of the earliest indicators of LCP disease[77].

MRI allows for noninvasive demonstration of morphological abnormalities of the femoral head typical of advanced disease, which may eventually lead to bone collapse and loss of epiphyseal sphericity, with joint deformity[78].

Small to moderate joint effusion and reactive synovitis are common findings in Legg-Calvé-Perthes disease. One of the earliest osseous abnormalities on non-enhanced MRI is nonspecific bone marrow edema pattern affecting the ischemic epiphysis (Fig. 23a&b), though hypointense signal may be present on T2-WI as well. Once necrosis is established, the affected bone usually displays low to intermediate signal intensity on T1-weighted images (T1-WI) and variable signal intensity in fluid-sensitive sequences; low signal intensity of the bone marrow in all sequences is indicative of advanced necrosis. The subchondral fracture appears as a curvilinear area in the anteroposterior

portion of the femoral head, with low signal intensity on T1-WI and variable signal intensity (usually hyperintense) on T2-WI[78].

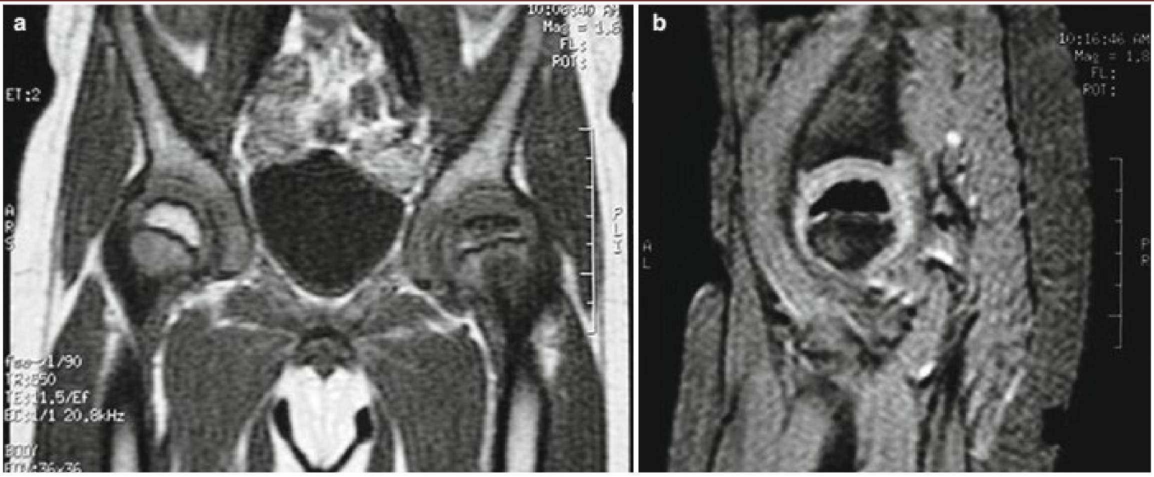

Figure (23a&b): Coronal T1-WI (a) and sagittal gradient-echo image (b) demonstrate reduced size and abnormal shape of the left proximal femoral epiphysis, with low signal intensity of the epiphyseal bone marrow in both sequences. There is thickening of the femoral cartilage, more evident in (a) [78].

B. Osteoarthritis:

Conventional X-rays remain indispensable for the diagnosis of osteoarthritis, while MRI is able to depict additional early symptoms and signs of activity of the disease. With the increasing number of joint-preserving interventions such as surgical hip sub-luxation and hip joint arthroscopy for treating femoro-acetabular impingement (FAI), high-resolution imaging is gaining further importance for both pre- and postoperative diagnostics because it can accurately recognize early stages of joint damage. With high-

resolution MR sequences and MR arthrography, the detailed depiction of the thin cartilaginous coating of the hip joint has become quite possible[79].

Virtually all the structures of a joint are involved in OA, and MRI is capable of delineating the morphology and to some degree the integrity of these tissues. Osteophytes are often more apparent on MRI than on radiographs. The cortex of the osteophyte and the marrow are continuous with those of the host bone, and these features are well demonstrated on MRI. Subchondral edema, sclerosis, and cysts can be seen. Edema-like signal produces areas of intermediate to low signal on T1-weighted or intermediate-weighted images and bright signal on fluid-sensitive sequences. Subchondral fibrosis and trabecular thickening replacing normal marrow (which contains fat) result in hemispherical subchondral areas that are intermediate in signal on T1-weighted images and intermediate to low in signal on T2-weighted images. Cystic changes may occur within the areas of subchondral sclerosis, producing well-defined regions that contain fluid signal [80] (Fig. 24:a-e).

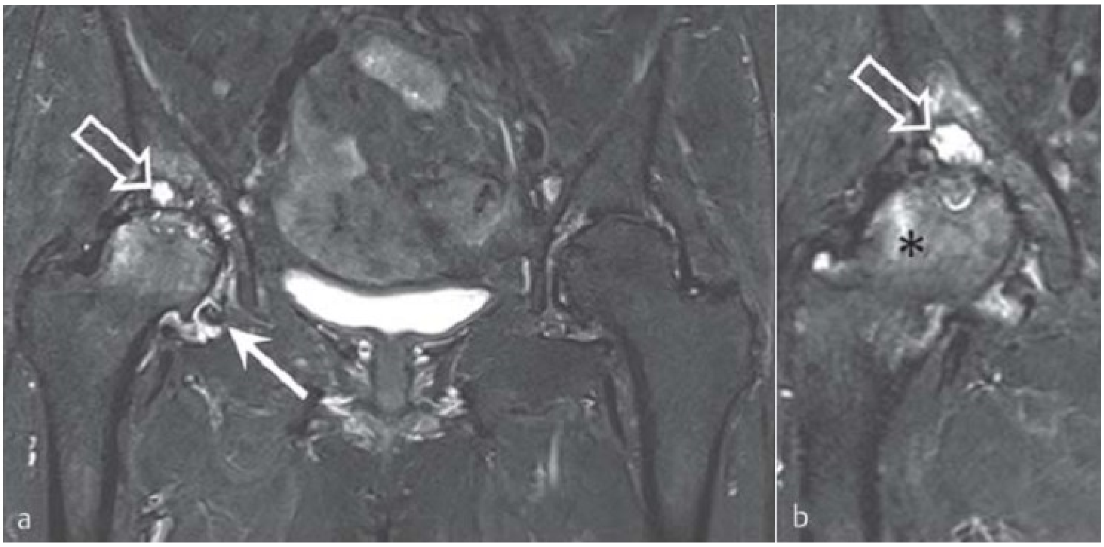

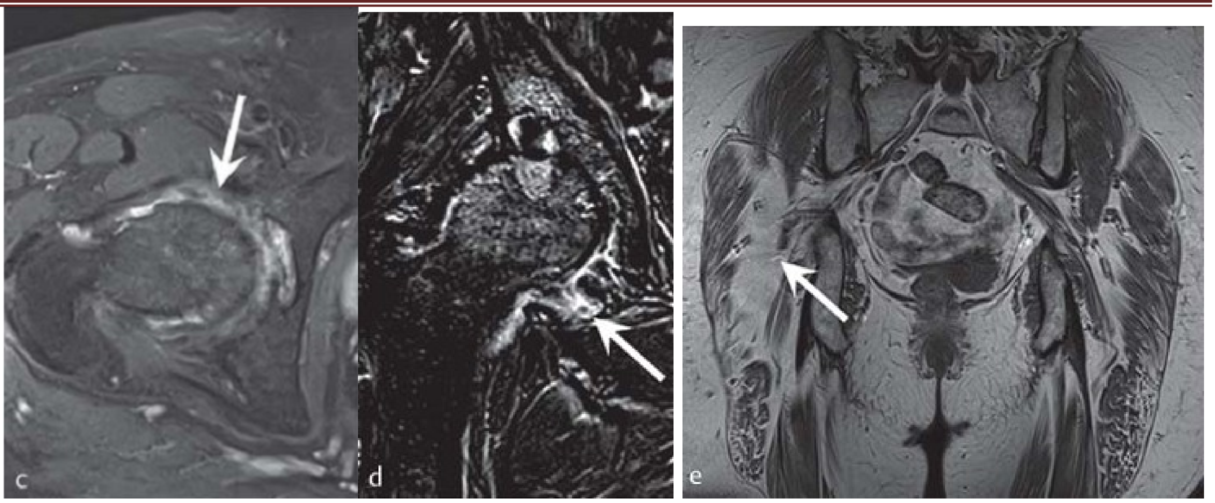

Figure (24:a-e): Activated right-side osteoarthritis in a 69- year-old female with bone marrow edema (asterisk) in the femoral head and acetabulum, subchondral cyst formation (open arrows), free body (arrow in a), synovitis (arrows in c–d), and fatty muscle atrophy (arrow in e) of the right-side gluteal muscles (a–b coronal STIR; c axial contrast-enhanced fat-saturated T1-weighting; d coronal subtraction (CE T1w – T1w); e coronal T1-weighting) (79).

Direct MR arthrography is the best imaging modality for preoperative evaluation of damage to the labrum or cartilage at the hip joint. Since there is often no presence of effusion with labrum lesions and the labrum may show a heterogeneous signal in healthy patients, too, distension of labral tears through direct MR arthrography leads to better diagnosis with a sensitivity/specificity of 90 – 95 %/91 %. [79].

Loose bodies are best visualized with T2-weighted images. Because of the lower intensity of repaired cartilage, it cannot be differentiated from the sclerotic subchondral region and thickened calcified cartilage. All those three parts are hypointense on T1- and T2-weighted images[81].

C. Inflammatory arthritis:

MRI of septic arthritis may be used to demonstrate early bone erosions and cartilage destruction. In addition to joint effusions, associated findings include synovial thickening and enhancement, septations, and debris within the joint. Uncomplicated septic arthritis may cause abnormal signal within the marrow on both sides of the joint secondary to reactive edema, which may be difficult to be differentiated from osteomyelitis. A secondary complication of septic arthritis includes soft tissue abscess, which demonstrates localized fluid collection with peripheral enhancement following gadolinium enhancement. Edema within periarticular structures or fluid collections in tendon sheaths will also show bright signal on T2-weighted images[57].

MRI and sonography can be useful tools in evaluating patients with early rheumatoid arthritis. Both imaging techniques can

detect pre-erosive synovitis. They can also identify early bone damage before it becomes apparent on radiography. Furthermore, MRI can be used to predict future bone damage[82].

MR imaging has demonstrated greater sensitivity for the detection of synovitis and erosions than either clinical examination or conventional radiography and can help establish an early diagnosis of rheumatoid arthritis. It also allows the detection of bone marrow edema, which is thought to be a precursor for the development of erosions in early rheumatoid arthritis as well as a marker of active inflammation[83].

MR imaging of bone erosions shows sharply marginated bone lesion with correct juxta-articular localization and typical signal intensity characteristics that is visible in two planes, with a cortical break seen in at least one plane. Signal intensity characteristics are as follows: (a) on T1 -weighted images, loss of normal low signal intensity of cortical bone and loss of normal high signal intensity of the bone marrow cavity, with enhancement after the administration of gadolinium-based contrast material; and (b) high signal intensity on T2-weighted and STIR images[83].

The pre-erosive lesions are indeed distinguishable from true erosions on MR images by their intact cortical margins and internal signal characteristics. On MRI, true erosions show cortical interruption and have well-defied, rounded margins and contain only synovial fluid or synovial tissue signal. In difference, these pre-erosive lesions have free water signal within the medullary space and tend to have somewhat ill defined margins. Also, unlike true erosions, they may appear to contain interspersed trabecular

bone or even fat[84].

MR imaging signs of synovitis include increased synovial volume (pannus), increased water content, contrast enhancement (increased signal intensity after the intravenous injection of gadolinium-based contrast material), or a combination of any of the above [83] (Fig. 25).

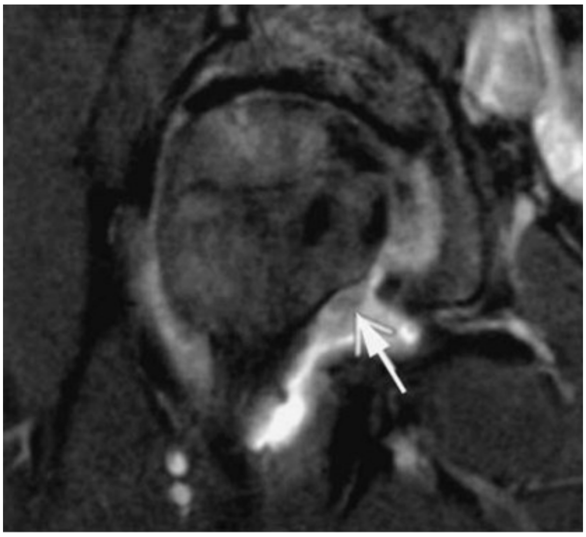

Fig. (25): MRI of the right hip joint (coronal, fat suppression, proton density-weighted): hypertrophic synovium (arrow) in rheumatoid arthritis[81].

D.Idiopathic Transient Osteoporosis:

Magnetic resonance imaging of Transient osteoporosis of the hip shows marrow edema involving the femoral head, neck, and sometimes intertrochanteric region with diminished signal on T1-weighted images, increased signal on fat-suppressed T2-weighted or inversion recovery MR images (Fig. 26:A,B&C), and contrast enhancement throughout the femoral head and neck, often associated with a joint effusion[85].

A  **B**

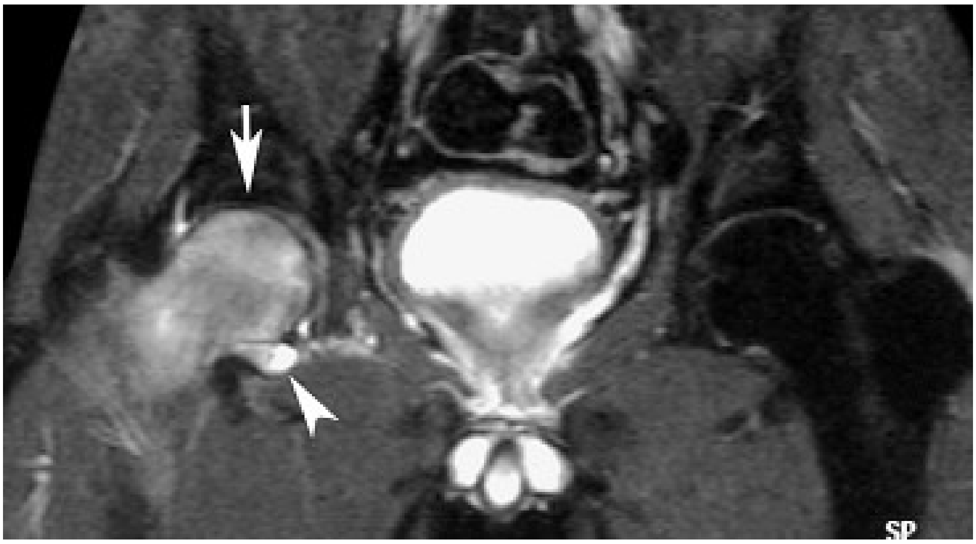

C

Figure (26:A,B&C): T1-weighted (A), T2-weighted (B) spin-echo MR images show diffuse low signal and high signal intensity, respectively, due to marrow edema. Coronal inversion recovery MR image(C) shows intense edema in the femoral head (arrow) and neck, and an effusion (arrowhead) [85].

On T1-weighted MR images, the bone marrow edema syndrome of the femoral head is characterized by an ill-delimited area of decreased signal intensity that consistently involves the femoral head and predominates in the subchondral area, frequently in the anterosuperior segment of the femoral head. The extent of the marrow changes is variable both in the head and in

the cervical region although epiphyseal involvement is the rule. Rarely, subtle marrow changes can be detected in the posterior aspect of the acetabulum[86].

On T2-weighted SE images, signal of the lesions becomes equivalent or higher than that of adjacent normal fatty marrow. The lesion lacks well-delimited lesions or margins. On fat-saturated intermediate weighted FSE images, the signal of the lesion is elevated and homogeneous[86].

Like skeletal scintigraphy, MR imaging may demonstrate findings positive for transient osteoporosis before the development of radiographic changes[87].

E. Developmental dysplasia of the hip

MRI provides morphologic information about acetabular deficiency in hip dysplasia. MRI measurements of center-edge angle using anterior to middle coronal MR images determined by triangulation with sagittal and axial images in which the femoral head forms a circle correlate well with radiographic measurements and can be used to assess acetabular deficiency (Table 8 and Fig.27A&B) [88] .

(Table 8):MRI Measurements of Developmental Dysplasia of the Hip [88].

Measurement	**Technique**	**Description**	**Normal Vs Abnormal**
Center-edge angle	Anterior to mid-coronal	Angle between vertical line through femoral head center and line tangential to lateral margin of acetabulum	Normal > 25° Borderline dysplasia = 20–25° Dysplasia <

Delta angle	Mid-coronal	Angle between lines drawn through medial edge of sourcil and superior edge of fovea capitis through	Normal > 10° Fovea alta ≤ 10°

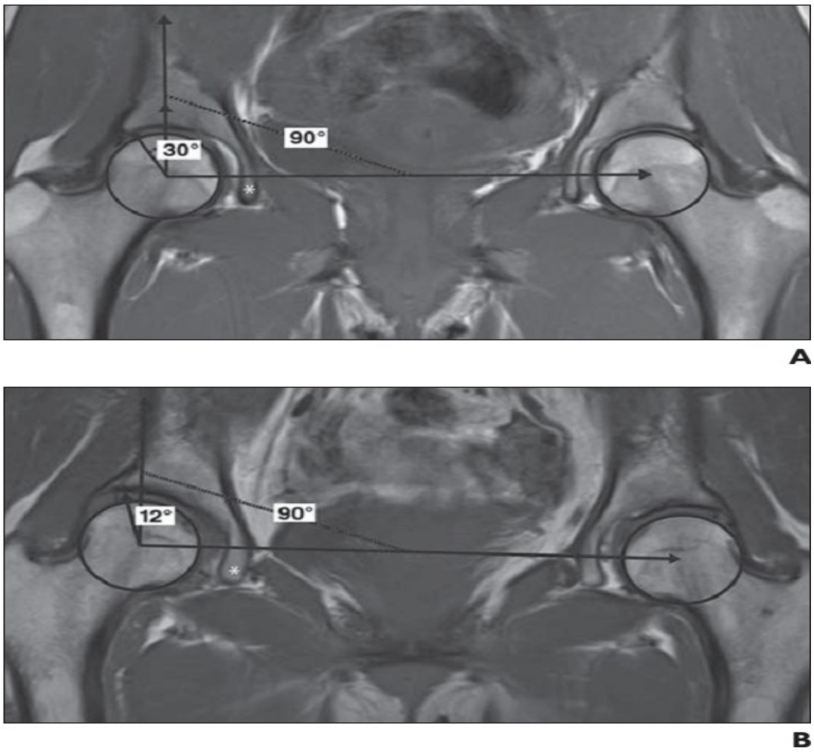

Figure (27:A&B): MRI measurement of center-edge angle. A and B, Coronal T1-weighted images of pelvis show measurement of center-edge angle as it is applied to MRI in 27-year-old woman (A) with normal center-edge angle > 25° and 32-year-old woman (B) with dysplastic hip with center-edge angle < 20°. Measurements are based on anterior or mid-coronal images of acetabulum determined by triangulation with sagittal and axial images where femoral head forms circle and teardrop (asterisk), which is well delineated [88].

MRI enables direct and accurate evaluation of the cartilage and important characterization of the cartilaginous acetabular angle. After successful reduction, the femoral head should be concentrically located in the acetabulum. The angle of abduction can be measured between the main axis of the femur and the midsagittal plane of the subject. This is important to note because too much abduction can lead to avascular necrosis. If contrast

material has been administered, the enhancement of the femoral head should be noted[89].

F. Fractures:

MRI is recommended for all symptomatic patients whose radiographic findings are negative for hip fracture. Diagnosis of minimally displaced hip fractures on radiographs can be challenging, especially in elderly patients with osteoporosis. In these patients, in the face of reasonable clinical suspicion for fracture, MRI is recommended for further evaluation when conventional radiographic findings are negative or equivocal[90].

Plain radiographs often show no apparent abnormalities in the early phase, so magnetic resonance imaging (MRI) should be performed immediately when subchondral insufficiency fracture(SCI) is suspected. One of the most characteristic MRI findings is a diffuse bone marrow edema pattern as well as a band-like low signal intensity lesion within the bone marrow edema pattern on T1-weighted imaging (Figs. 28;A,B&C and 29;A&B). This band lesion is the most distinctive finding and is essential for the diagnosis of SIF, which histopathologically corresponds to a fracture line with associated repair tissue. In addition, the shape of this low intensity band, usually irregular, serpiginous, parallel to the articular surface, and often discontinuous, is useful for the diagnosis (Fig. 30;A&B)[91].

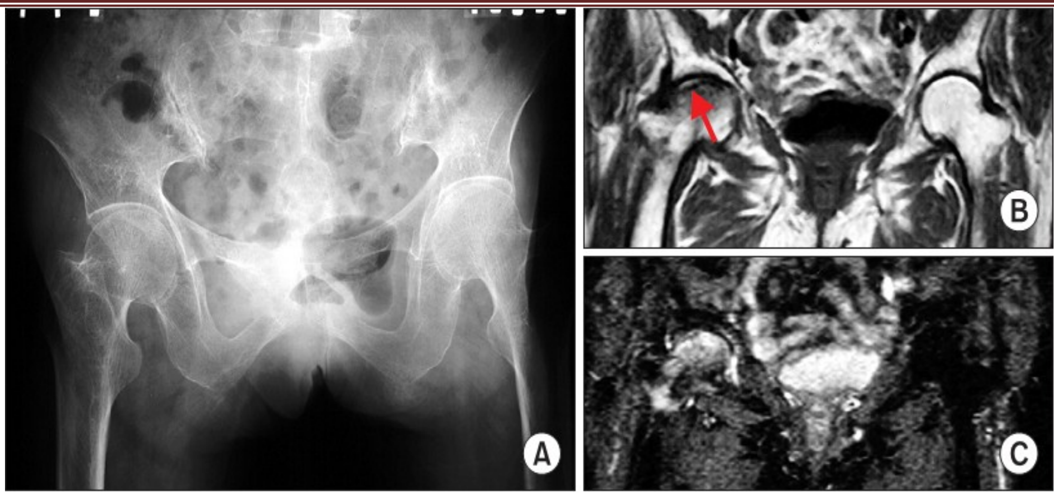

Figure (28;A,B&C): A 68-year-old woman with a subchondral insufficiency fracture of the right femoral head. (A) Radiograph obtained 4 weeks after onset shows no apparent abnormalities in the femoral head. (B, C) On magnetic resonance imaging obtained 4 weeks after onset, a diffuse bone marrow edema pattern is seen, with low signal intensity on T1- weighted imaging (B) and high signal intensity on T2-weighted fat saturated imaging (C). A very low signal intensity band parallel to the articular surface is also seen at image(B) (arrow) [91].

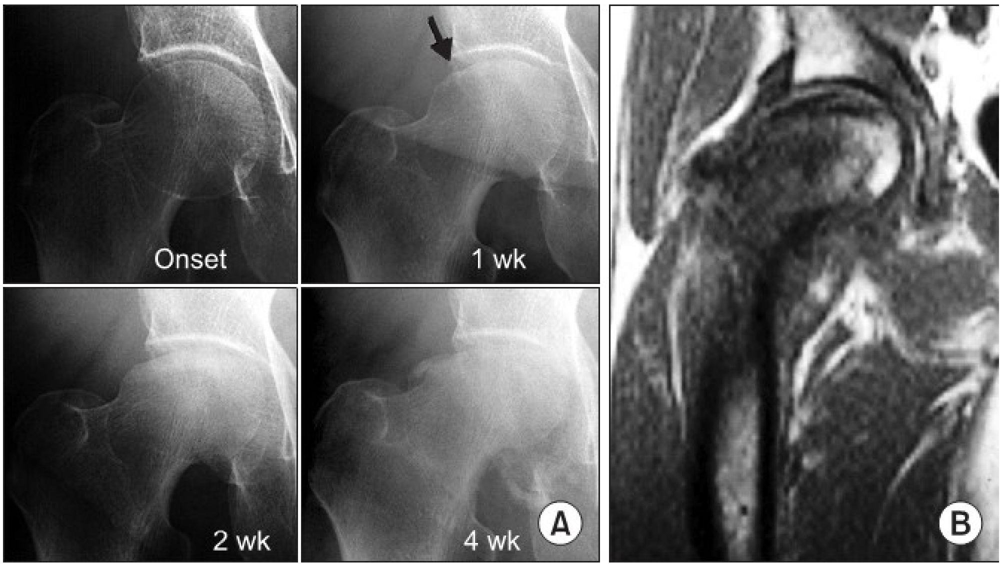

Figure (29A&B): A 59-year-old woman with a subchondral insufficiency fracture of the right femoral head, which resulted in rapid destruction of the hip joint. (A)No apparent abnormality is seen on the radiograph obtained immediately after the onset of pain. However, a slight collapse was seen on the lateral side of the femoral head 1 week after onset (arrow). The collapse progressed until 4 weeks later, when joint space narrowing, particularly on the medial side, is seen and rapid destruction of the femoral head is observed. (B) Magnetic resonance imaging 2.5 weeks after onset shows a bone marrow edema pattern with

two irregularly shaped low intensity bands with a convex shape on T1-weighted imaging [91].

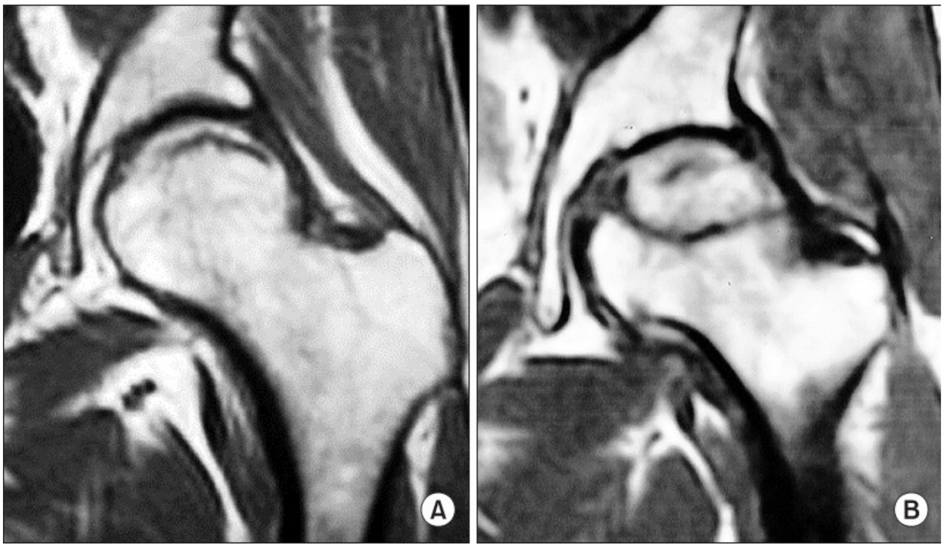

Figure (30A&B): Comparison of band images in subchondral insufficiency fracture(A) and osteonecrosis (B). Since the band in SIF corresponds to the fracture line, the shape is usually irregular, disconnected, convex and parallel to the cartilage surface. In contrast, the band in osteonecrosis corresponds to repair tissue formed around the necrotic area, which tends to show a smooth, well delineated and concave shape [91].

On T2 or gadolinium enhanced images, both the low intensity band and the area between the band and the articular surface tend to show high signal intensity, especially in the early phases of the fracture (Fig. 31;A,B&C) [91].

As the disease progresses, subchondral collapse of the femoral head may occur, but subsequent resolution of the low-intensity band with complete preservation of the femoral head may be observed[92].

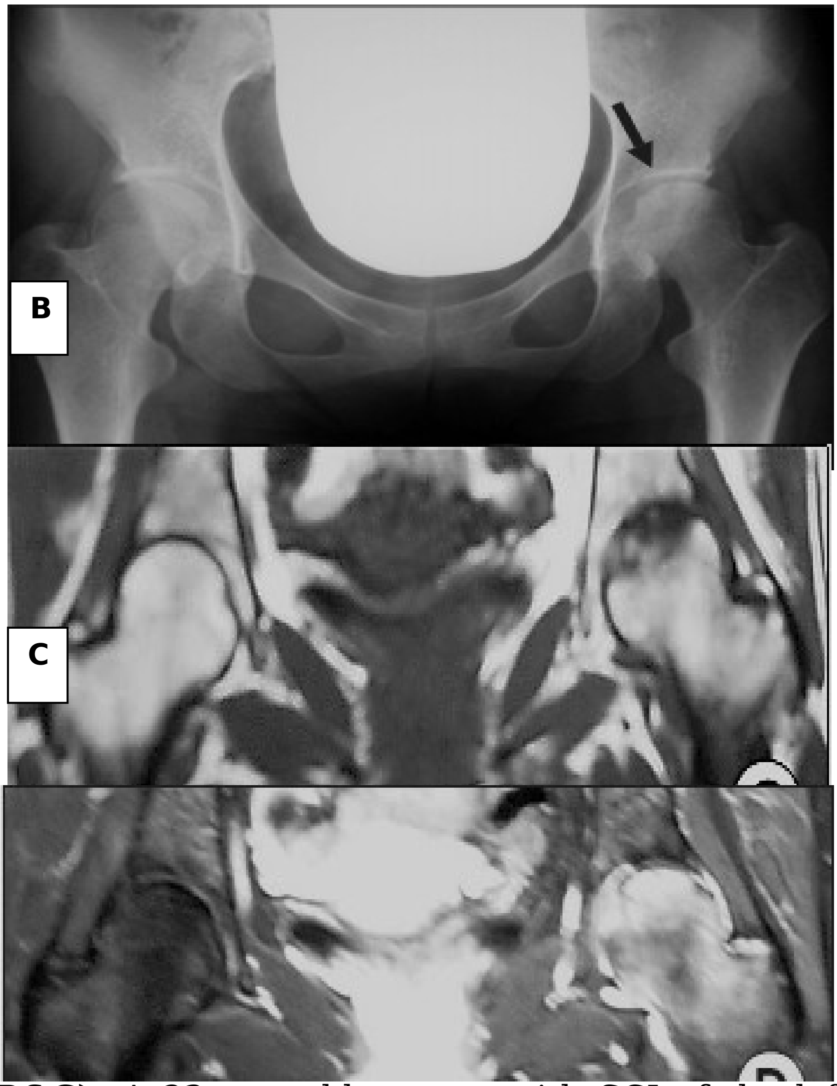

Figure (31;A,B&C): A 23-year-old woman with SCI of the left femoral head. (A) Radiograph obtained 2 months after onset shows slight collapse in the lateral portion of the femoral head (arrow) where an irregular joint surface and partial sclerosis are also observed. (B) A low signal intensity area and a band-like pattern are seen on a T1 weighted image. (C) On gadolinium enhanced magnetic resonance imaging, the lesion totally shows diffuse high uptake, indicating that this area is alive. A bone biopsy was performed

and the final histopathological diagnosis was subchondral insufficiency fracture in young age [91].

MRI plays a role in the detection of the early occult SCFE with normal plain radiographs. In these cases, MRI demonstrates epiphyseal plate widening, adjacent bony edema, joint effusion, and synovitis (Fig. 32;A,B&C). MRI has a limited role in the presence of radiographic evidence of deformity. MRI may play a role in the detection and characterization of subsequent osteonecrosis[93].

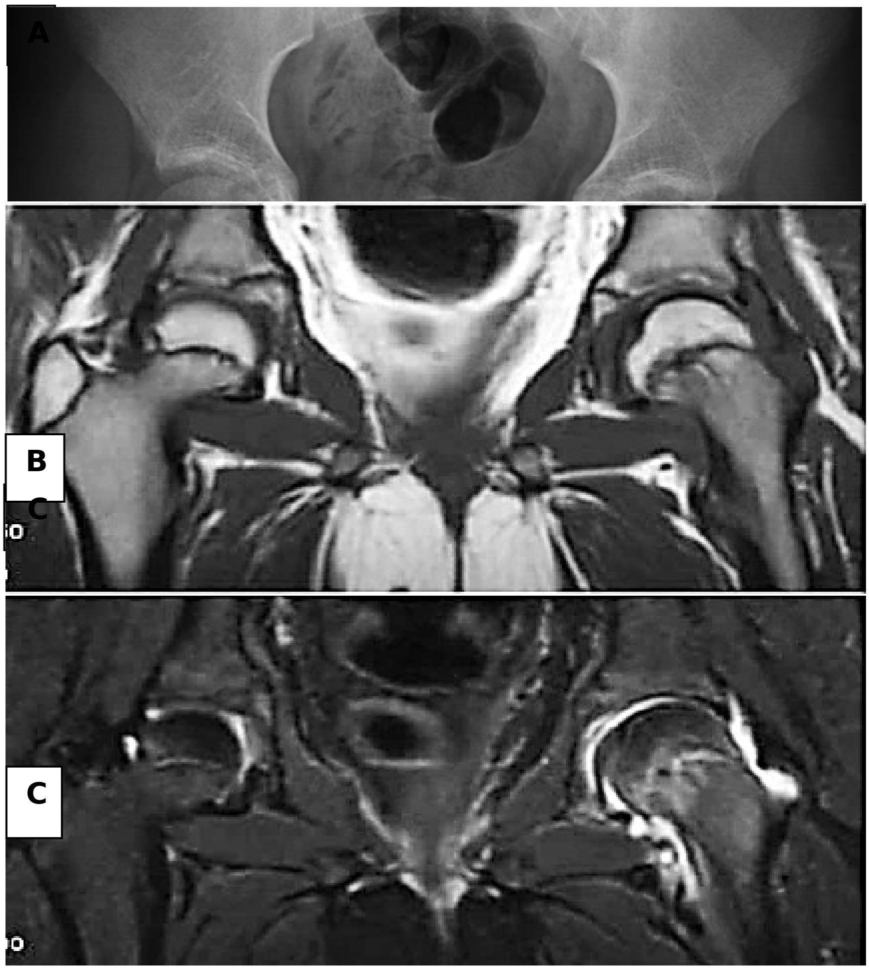

Figure (32;A,B&C): (A) Plain radiographs show minimal evidence of a SCFE. (B) The T1 weighted image shows some

epiphyseal widening in the left hip. (C) The T2 weight image shows edema around the epiphyseal plate [93].